Generation and characterization of 12th harmonic out of 1025nm femtosecond Yb:YAG laser

Dmitry Anatolievich Zimin, Ruhr University Bochum, Germany

September 9, 2015

Abstract

Generation of 12th harmonic of 85nm by means of non-linear optical effects was investigated. Active medium of solid state BBO crystals as well as gas medium of Ar, Kr, Xe was used. Beam characterization of 85nm harmonic was performed.

Contents

1 Introduction

This is a report for the work which has been performed during the "DESY Summer School 2015" program at the "DynamiX" group of femtosecond X-ray physics. The work was supervised by Dr. Marek Wieland and Dr. Armin Azima and revised by the head of the group Prof. Dr. Markus Drescher. In addition, I would like to thank Dimitrios Rompotis for theoretical support.

2 Theory

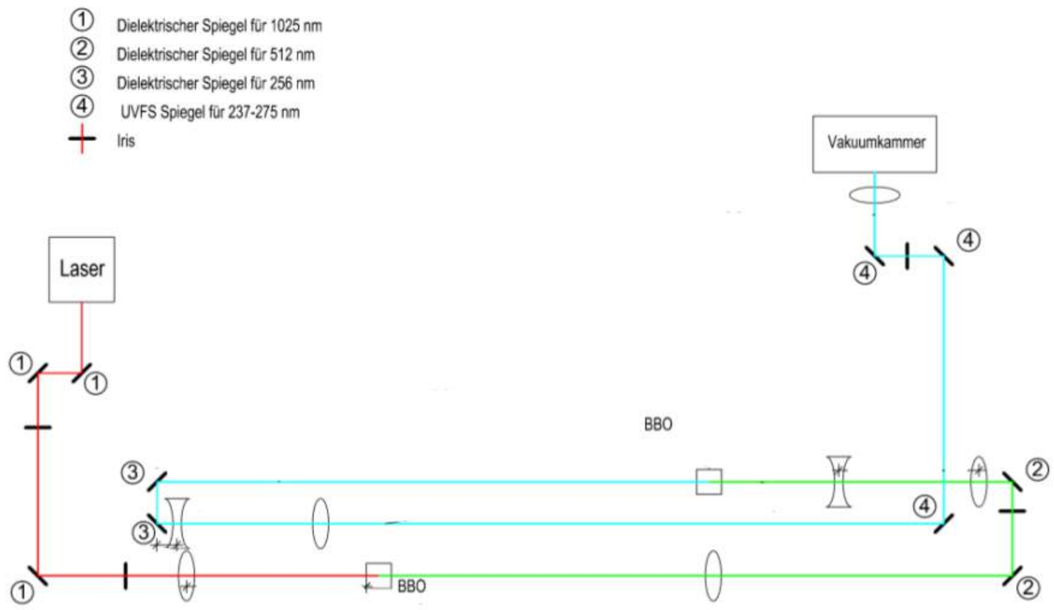

Figure 1: Experimental setup [2]

The experimental setup used for measurements is shown on Fig. 1. Commercial femtosecond laser JenLas D2.fs [1] was used as a fundamental harmonic. The fundamental wavelength of 1025nm was incident on the first BBO crystal. Due to the appropriate alignment of the birefringent crystal, phase matching condition is being fulfilled, hence generating a second harmonic of 512nm. The generated harmonic is even due to the symmetry of the solid state crystal which allows generation of even harmonics only.

After second harmonic generation, dichroic mirror for 512nm was placed which allowed to omit the fundamental harmonic of 1025nm and reflect only generated second harmonic. The same procedure was used with the dielectric mirror for 256nm to eliminate 512nm harmonic after the second BBO crystal. Therefore only fourth harmonic of 256 was entering the vacuum chamber.

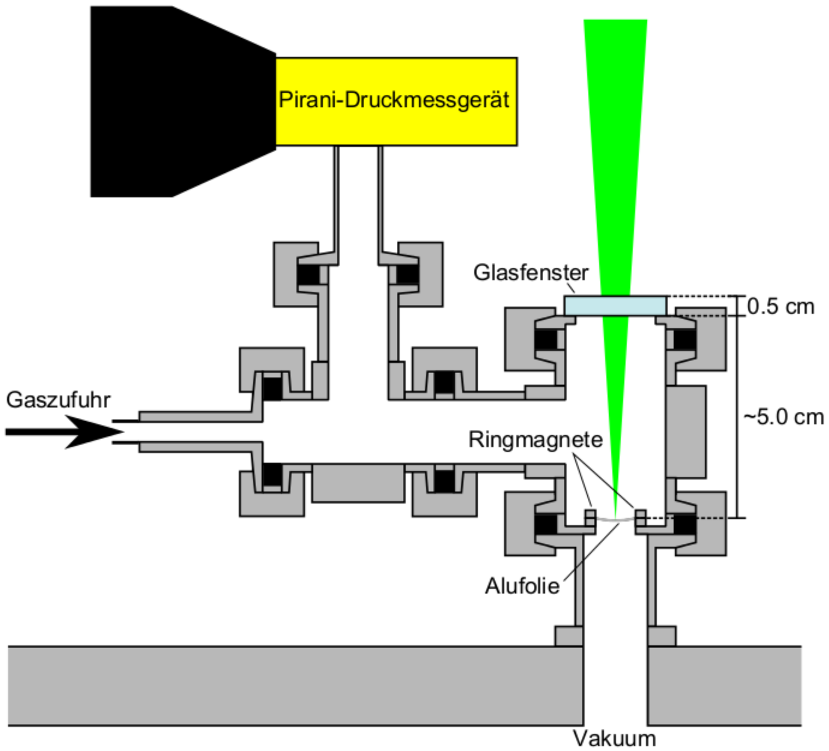

Figure 2: Setup of the gas chamber [3]

Following the fourth harmonic generation, the light of 256nm wavelength is entering the gas chamber separated from the main vacuum chamber by the thin aluminum film as depicted on Fig. 2.
The relatively high intensity of the generated fourth harmonic and absorption spectrum of aluminum in the UV range allows to burn the hole in the film as the focusing plane of the lens used before the gas chamber window approaches the plane of the aluminum film.
The purpose of the gas chamber is to create a relatively high density of gas molecules which act as an active medium for 12 harmonic generation. Due to the symmetry of the potential of the gas molecules only odd harmonics can be generated. Therefore from 256nm due to non-linear optical effects it is possible to generate 85nm, 51nm etc. 85nm have been indeed observed, however higher harmonics have not been detected.
In fact, the actual non-linear effect responsible for the harmonic generation in the gas in our case is a multiphoton absorption. According to Heisenberg uncertainty, energy and time are conjugate variables (Eq. 1).

$$\Delta E \Delta t \geq \frac{\hbar}{2} \tag{1}$$

Hence, Rydberg energy levels of used for the experiment noble gases (Ar, Kr, Xe) become spread as time becomes more localized. Since used for the setup laser provides pulses with the pulse period of less than 400fs, which is a relatively short time, Rydberg energy

levels become delocalized providing possibility to excite an electron into the ”band” of energy levels, however this ”band” is not homogeneous in terms of lifetimes of each energy in particular as a consequence of Heisenberg uncertainty.
Therefore for the case of spectrum of Argon, it can be seen that if 3 photons of 256nm are combined due to multiphoton absorption non-linear effect, the total energy of 3 photons is equal to 14.586eV which corresponds to approximately 3p Rydberg level. Since there is an uncertainty in energy, then for the short time it is possible to excite electron from the ground state into the energy level with energy approximately equal to the Rydberg level. As the electron then decays spontaneously to the ground state level, which does not violate transition rules, photon with the energy equal to triple photon energy of 256nm is emitted, which corresponds to 85nm.
Although it is not completely clear why higher than 85nm harmonics were not observed, the explanation might be that, the energy of 5 photons of 256nm wavelength is higher than ionization energy of Argon, therefore instead of generation of 5th harmonic the atom is likely to be just ionized. Hence the probability for the higher than 85nm harmonic generation should be quite low.
Efficiency of the higher harmonic generation is a function of intensity of the light by which the medium is being exposed, but also of the density of the gas molecules, as there is a need to localize 3 photons and gas molecule at the same time and the same place. The higher the intensity of the incident light and the higher the density of the gas molecules, the higher is the probability for generation of the higher harmonic.
Hence the intention is to produce as high as possible intensity for the 4th harmonic of fundamental, and create as high as possible gas density in the chamber. However it should be mentioned that too high density, has also negative effect as in this case emitted photon of 85nm can be observed by the neighboring molecule which will then scatter the light. Therefore the amount of photons reaching the vacuum chamber reduces.
The purpose of the vacuum chamber is to separate XUV radiation from air, as it will be absorbed by the air molecule s.

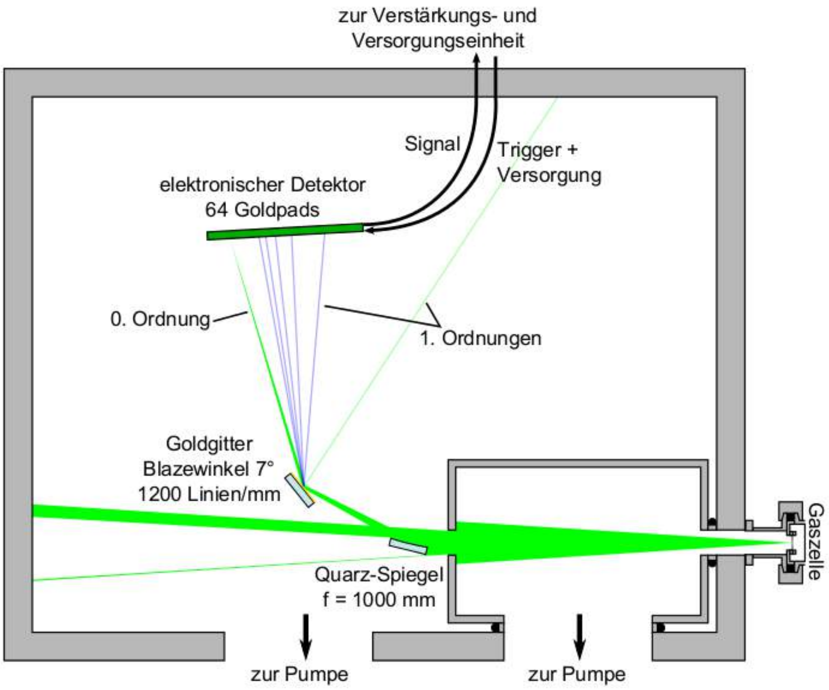

Figure 3: Setup of vacuum chamber [3]

Generated photons of 85nm pass through the hole burned by the laser to the vacuum chamber (Fig. 3) and incident on the quartz lens which act as a mirror. Since for SiO_2 material the reflectance strongly depends on the incident angle as shown on Fig. 4, the lens is tilted to increase the reflectivity from the surface of the lens and therefore use it as a mirror.

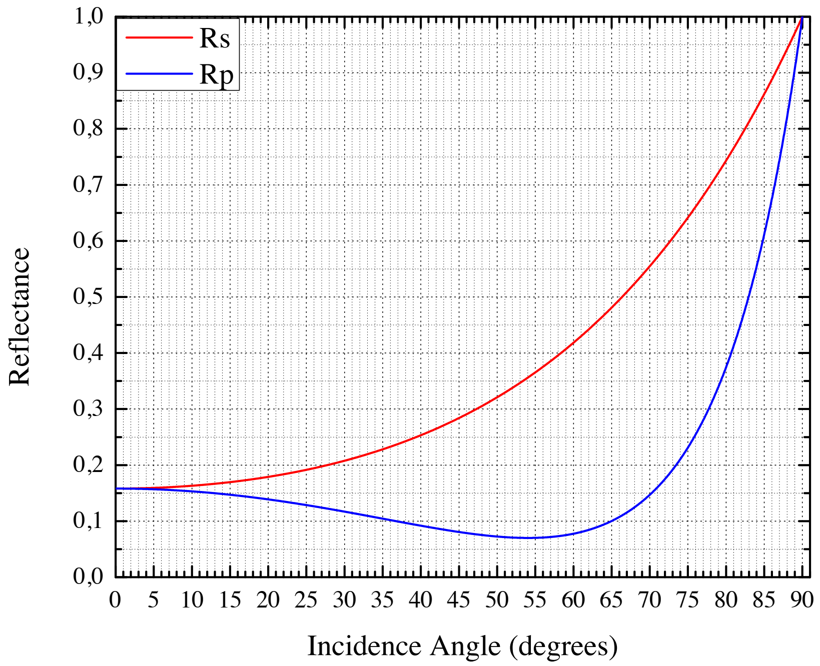

Figure 4: Reflectance of SiO_2 for 85nm wavelength [4]

Reflected beam is then incident on a blazed diffraction grating causing 256nm and generated higher harmonics to be deviated by different angles and hit the detector which consists of 64 pads.
By knowing the position of the 0th mode of the grating on the detector, or the position of the first mode of the 256nm and geometry of the setup, using the grating equation (Eq. 2) it is possible to calculate which position on the detector corresponds to which wavelength diffracted from the grating.

$$sin(\alpha) - sin(\beta) = \frac{m\lambda}{d} \tag{2}$$

α - angle of incidence, β - angle of diffraction, λ - wavelength, d - line spacing of the grating, m - order of diffraction

One has to also consider the attenuation of a intensity of the light incident on a diffraction grating due to absorption of the grating (Fig. 5).
The typical signal observed on the oscilloscope is presented on Fig. 6.

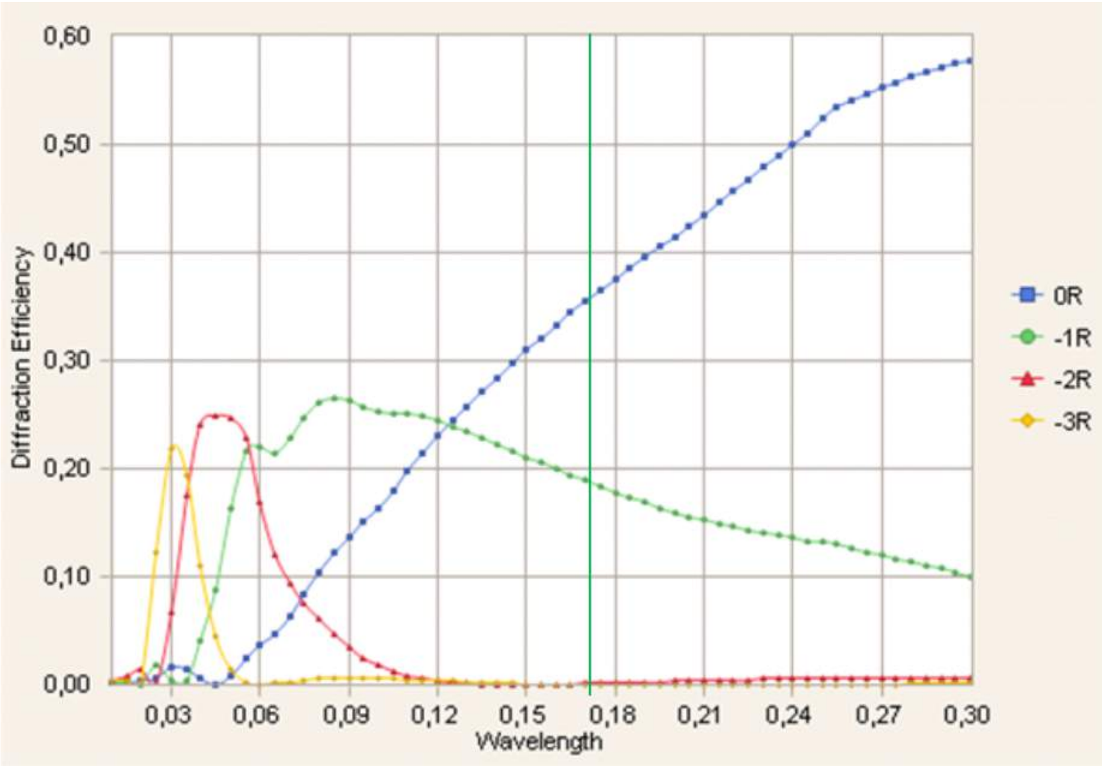

Figure 5: Efficiency of diffraction grating for different wavelengths [3]

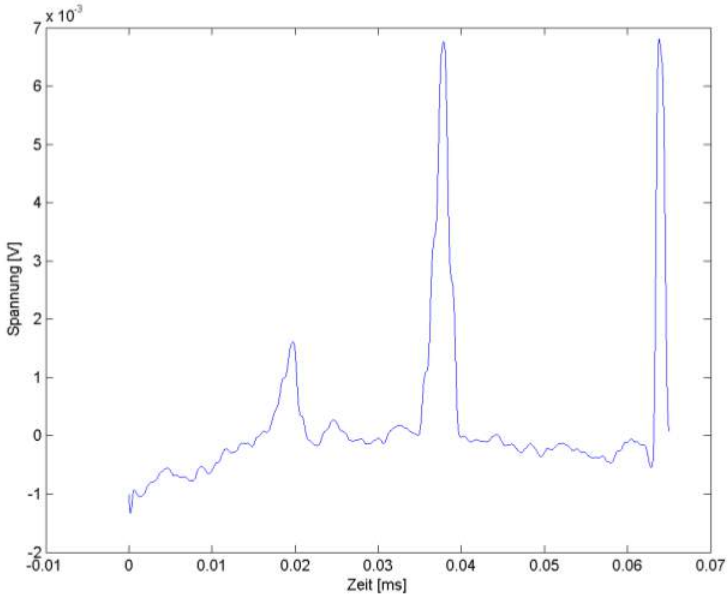

Figure 6: Signal on the detector [2]

After the processing of the signal one can map the number of the pad of the detector to the diffraction angle from the grating (Fig. 7).

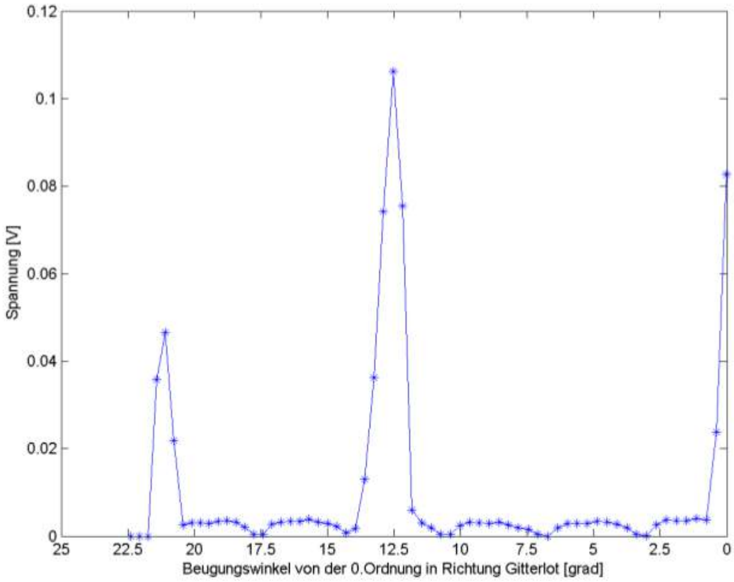

Figure 7: Map of the pads on the detector to the diffraction angles from the grating [2]

However in some occasions multiple peaks were observed (Fig. 8). The cause of the multiple peak formation can be quite different and at a first glance it is not clear what is the reason for such a multiple peak formation. Whether it is a spectral effect which can be explained by means of non-linear optics, effect of the beam profile or effect of some stray lights in the setup etc.
The main purpose of this work was to investigate and explain this phenomenon.

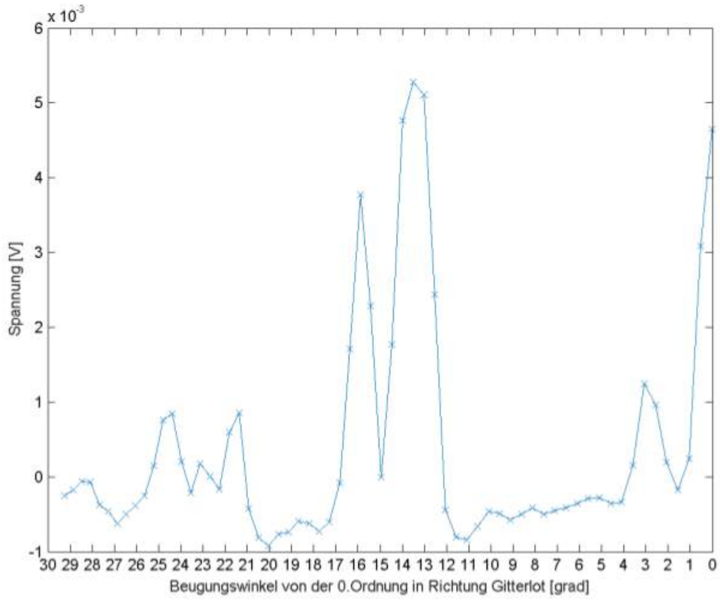

Figure 8: Map of the pads on the detector to the diffraction angles from the grating [2]

3 Measurement

3.1 Hole investigation

On Fig. 9 one can observe the hole with rings, which suppose to be diffraction rings, from used optical components. Such a pattern was observed only once, and probably occurred due to diffraction from one the used apertures in the setup or other optical components.

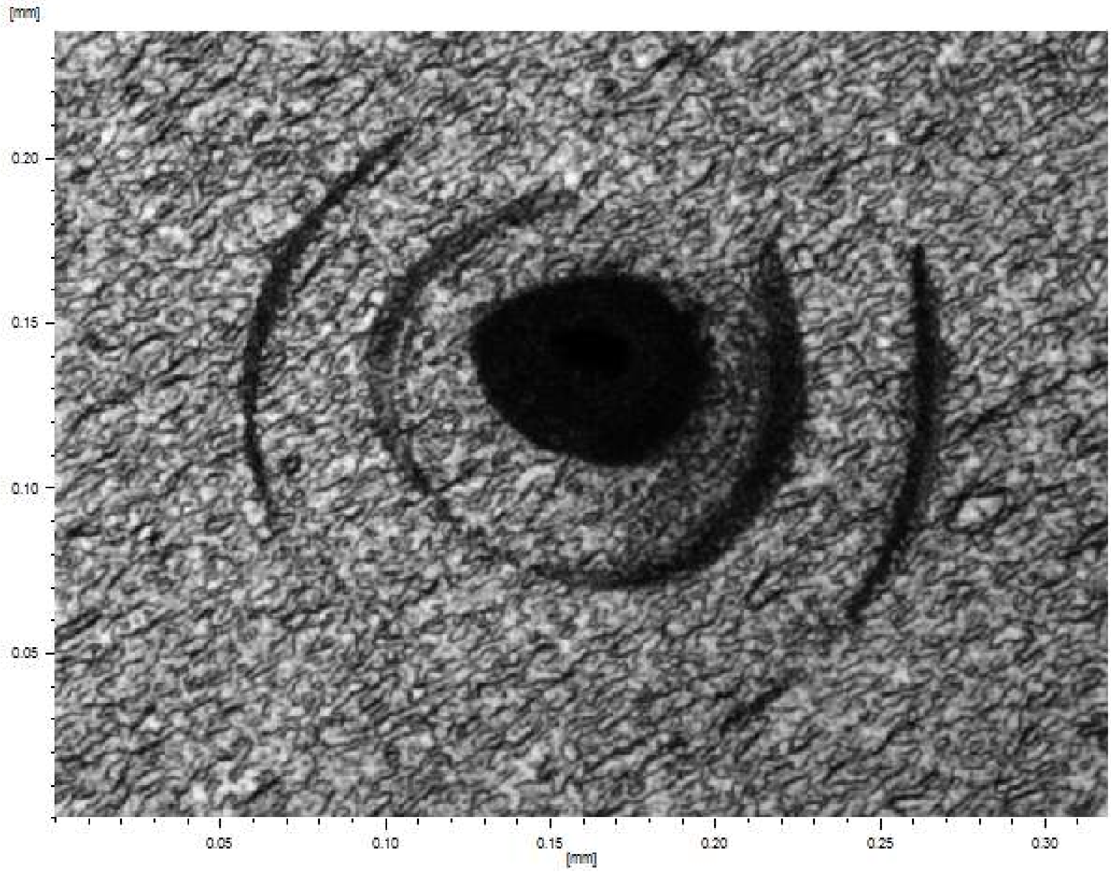

Figure 9: Pumping current 38A. Operational time about 1 hour

The minimum pumping current of the laser need to provide enough intensity for 4th harmonic was found to be less than 24A. At 24A it is still possible to burn the hole, smaller amounts of pumping current were not tested.
By moving the focal plane to the film plane from both sides it is possible to find out that using 75mm focal distance converging lens and 38A pumping current the maximum mismatch of the focal plane and foil plane which still allows to burn the hole is about 237,5um to each side from the foil plane, this number it fact is related to the Rayleigh length of the 4th harmonic. Hence the total interval which allows to burn the hole is about 475um.

In fact by determining the positions where the hole is burned while approaching the focal plane to the foil plane from both sides it is possible to precisely determine the position where the foil plane exactly coincides with the focal plane, as the middle point of the interval between these two positions. Hence it was possible to measure the diameter of the hole at the focal plane (Fig. 10).

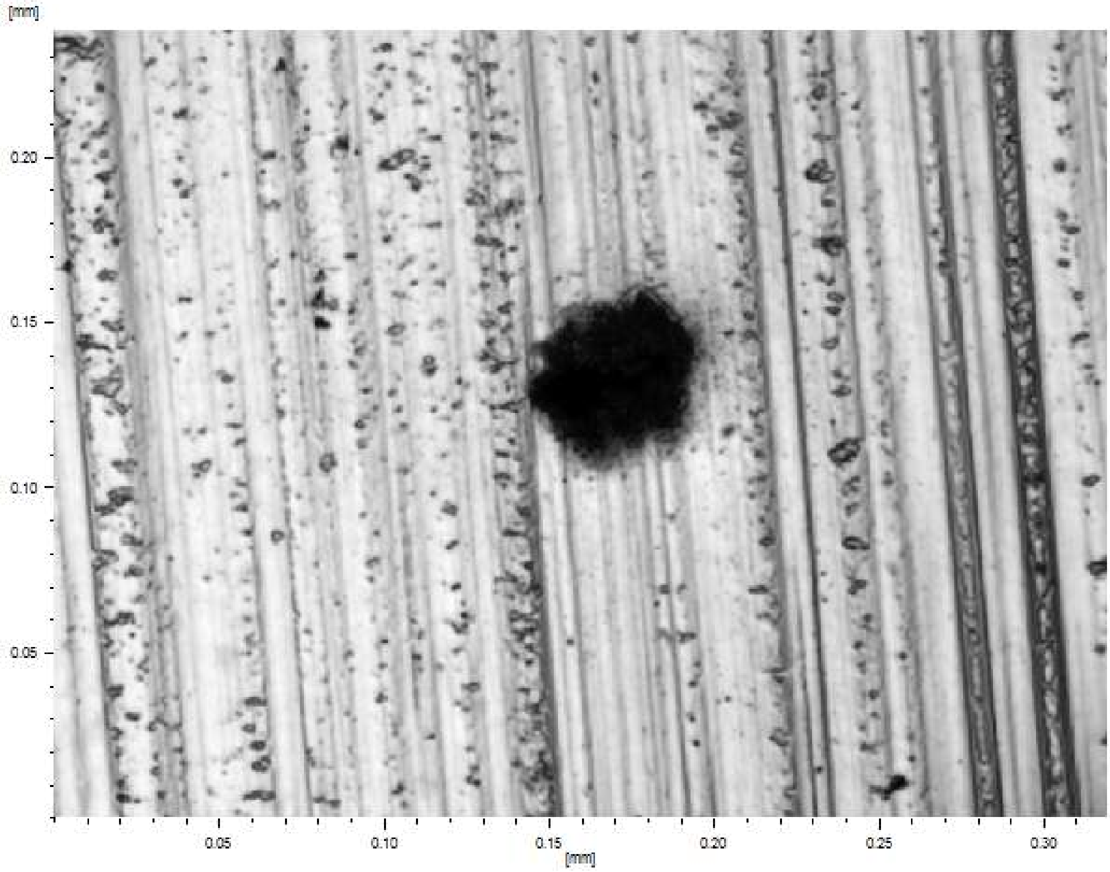

Figure 10: Diameter of the hole at a focal plane of 75mm lens after operation time of about 30 min

However at the short operational time of about 20 seconds one can observe the actual hole and melting area due to the jitter of the laser and heating. This implies that the shape and dimensions of the hole change as operational time increases, hence corresponds to the decrease of the pressure in the gas chamber and lowering of density of gas molecules which should reduce the efficiency of harmonic generation ((Fig. 11)).

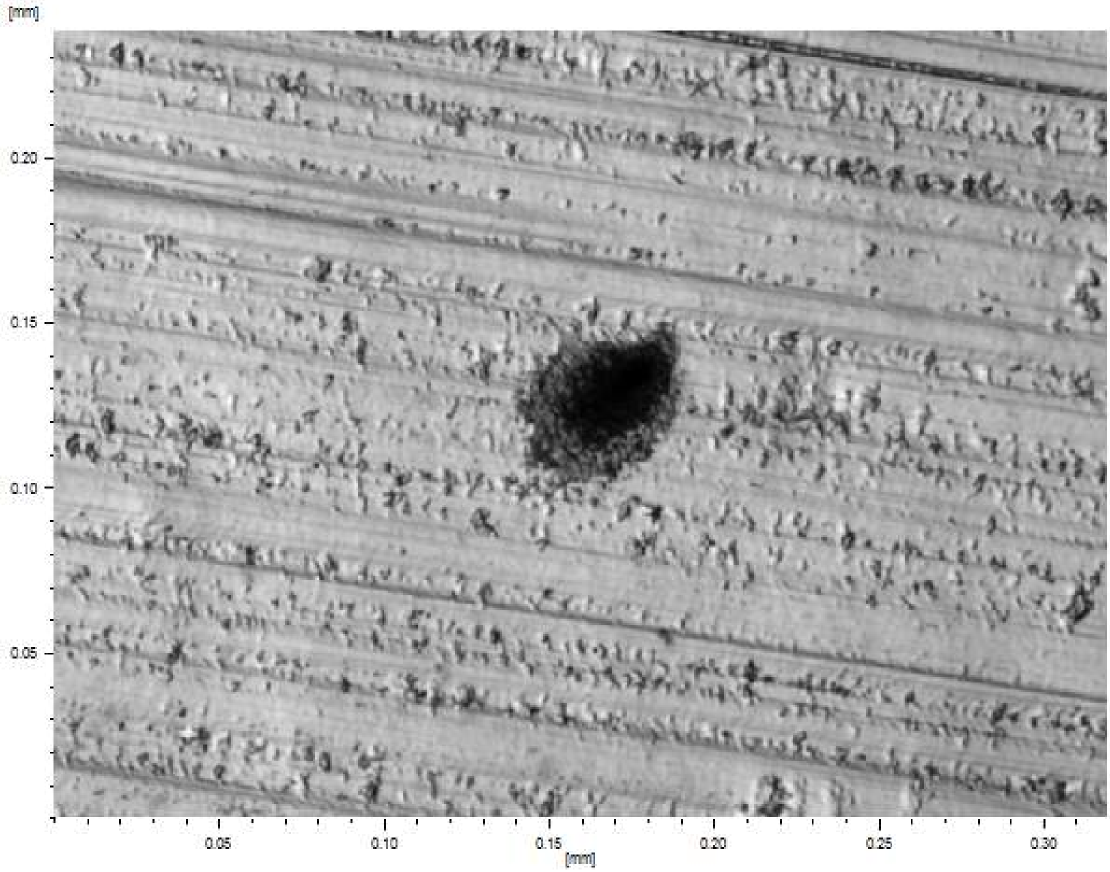

Figure 11: Diameter of the hole at a focal plane of 75mm lens after operation time of about 20 seconds

The experiment to record the change of the signal as a function of operational time due to expansion of the hole was conducted, but no noticeable changes were detected, this, however due to the fact that the detector was saturated, while the problem of saturation was not known at that time.
In addition the presence of the gas chamber window shifts the position of the focal plane comparing to the position without the gas chamber window. The effect of the gas chamber window was found to produce a shift of the focal plane of about 60um.
It was also observed that the position of the film in air shifts for about 1mm with respect to position of the film when the vacuum chamber is evacuated and gas chamber is pumped with gas, due to the pressure difference.

3.2 Divergence measurements

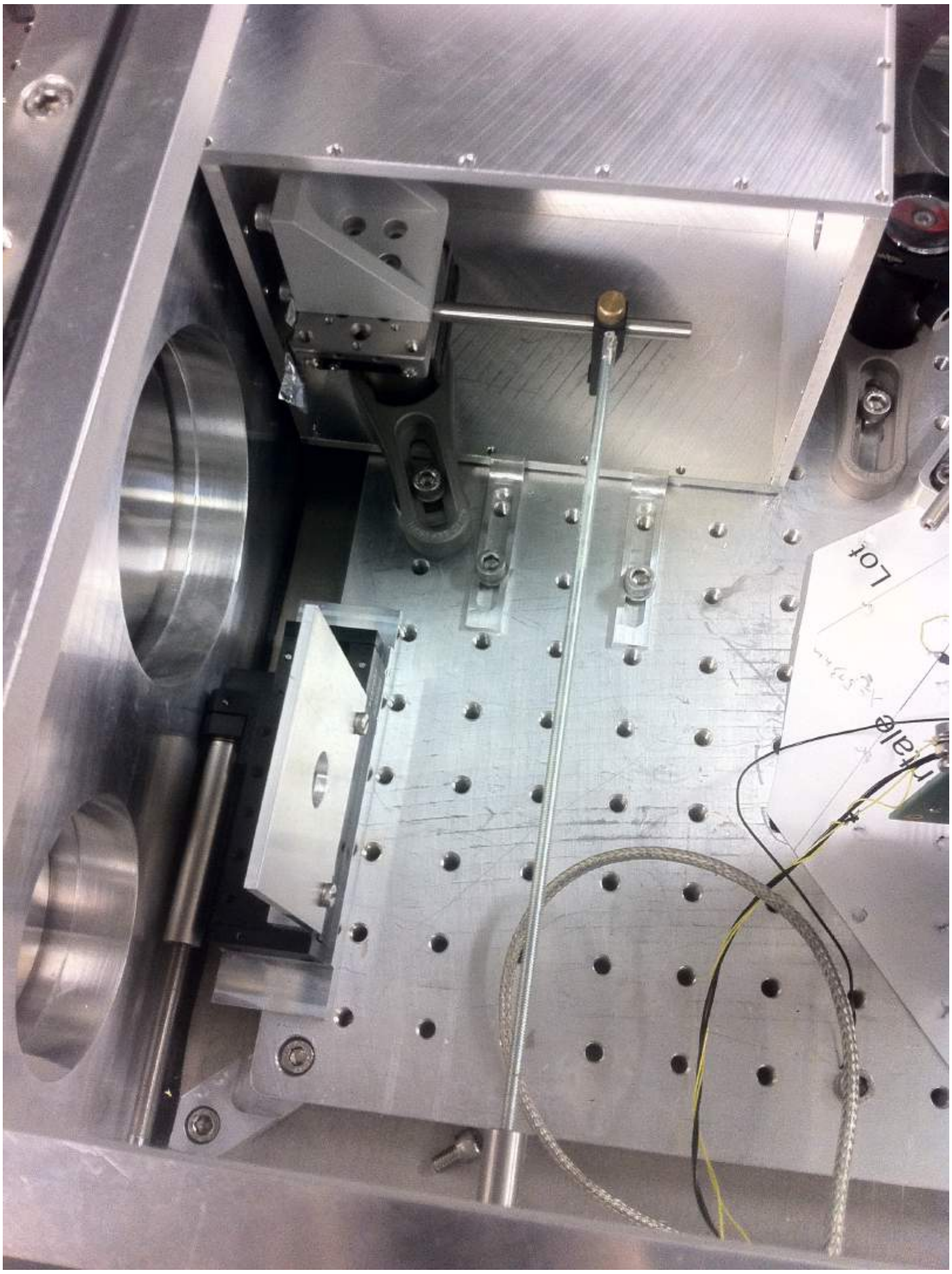

Figure 12: Full setup for divergence measurement

In order to measure the divergence the structure of moving stages with attached blade has been assembled. The blade and the moving stages were covered by the aluminum

foil painted by the graphite spray in order to prevent potential reflections.
The bulk solid stick was attached to the micrometer of the chamber from one side and to the blade on moving stages to the other side in order to convert rotational movement of micrometer to the translational movement of the stick. The stick will then push the blade on a moving stage across the beam profile (Fig. 12).
The profile measurements were done at two positions which allowed to calculate the divergence. The first experiments were rather unsuccessful due to the number of properties of the setup which were not known at that time. In particular, pad detector experience a saturation, therefore measurements are possible only in a range of up to 25A of diode pumping, as for the higher pumping current the signal becomes saturated. The diameter of the beam of 85nm harmonic at the plane of the mirror which is suppose to reflect the light on the diffraction grating is greater than the surface of the mirror exposed by light. Therefore the mirror collects only a part of the beam, and moreover, depending on the position of the mirror, different parts of the beam are reflected to the grating, this makes signal to be dependent on the position of the mirror with respect to the beam profile. Background signal on the detector changes with time and the diameter of the hole extends with time. Since the precise profile measurements were taken about 1hour each, the conditions for the experiments at the beginning of the measurement and at the end were not the same.
However after these problems were discovered the second try of divergence measurements were performed, were all mentioned above effects were taken into account.
The intention of the measurement was to measure the position of the blade when the peak is just started to be affected by the blade (the beam is cut by about 5 percents comparing to saturated peak), means saturation is avoided, and the position where this peak is almost disappear (signal becomes about 5 percents of the original signal). (Fig. 13, 14, 15, 14). By doing so we effectively measure the signal in the region between saturation and absence of the signal, as a function of the position of the blade.

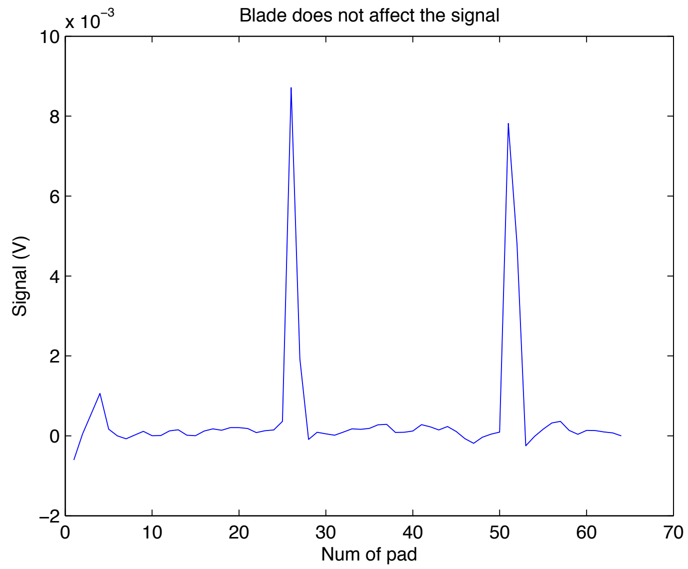

Figure 13: Signal before cutting the beam. 1st position of the blade.

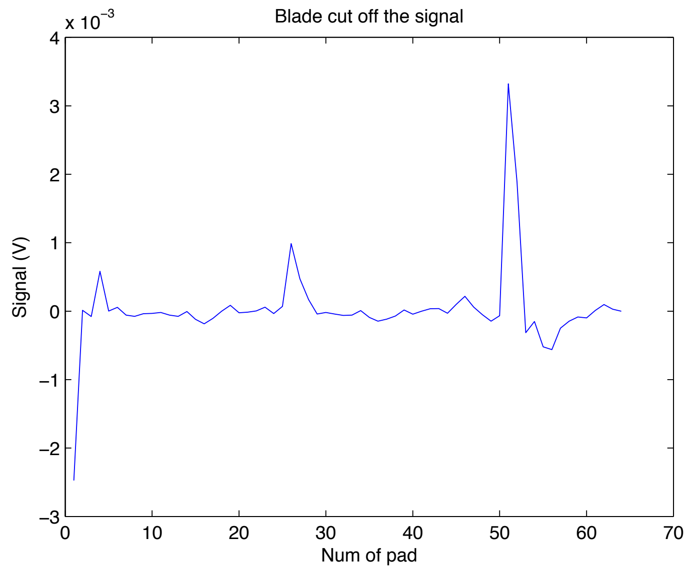

Figure 14: Signal after cutting the beam. 1st position

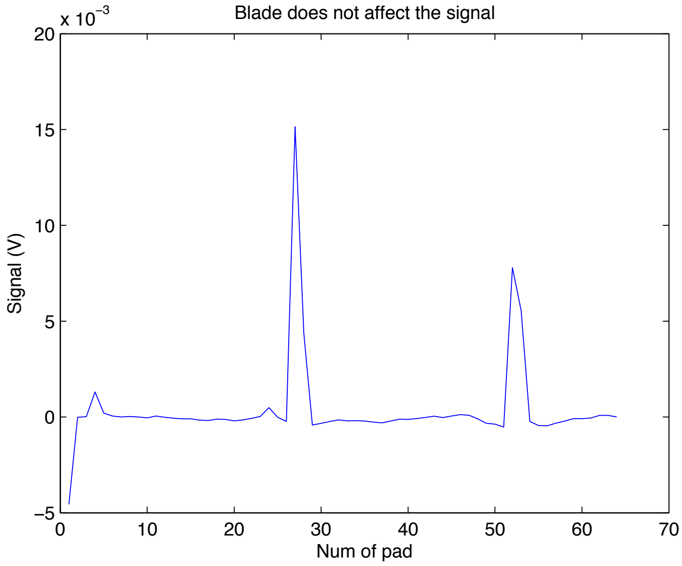

Figure 15: Signal before cutting the beam. 2d position of the blade.

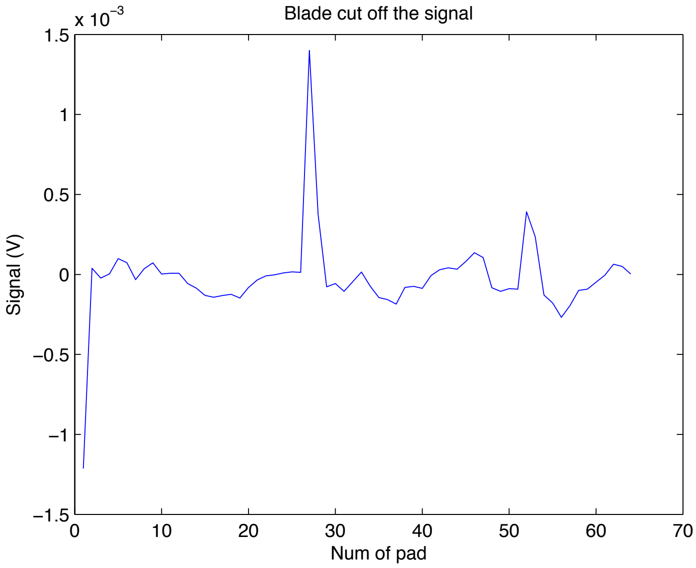

Figure 16: Signal after cutting the beam. 2d position

The difference between two positions of the blade was 82,19mm. The distance the blade has to be moved to almost close the peak was 0.276mm in the first experiment and 3.408mm in the second.

$$\Theta = 2 * arctan(\frac{D_2 - D_1}{2L}) \tag{3}$$

Using the Eq. 3 for divergence, where L is a distance between positions of two measurements, D_1 and D_2 are distances the blade moved perpendicular to profile, one can derive that the divergence is approximately equal to 4.37 degrees.

It should be mentioned, that this divergence value can not be considered fully accurate, because only the part of the beam was considered and only along one axis. However for the actual divergence the entire diameter of the beam has to be known.

3.3 Profile measurement without mirror

One of the experiments for profile measurements was done without usage of the lens acting as a mirror (Fig. 17). The grating and the detector were placed such that the 0th order beam from the 4th harmonic (256nm) was just a little touching of the most right pad on the detector, while the 1st order of the 256nm harmonic was barely touching the most left pad on the detector. In this case expected 1st and 2d orders of the generated 85nm harmonic must incident on a surface of the detector. The pads of the detector were covered by the white stripe in order to block most of the pads surface and act as a point.

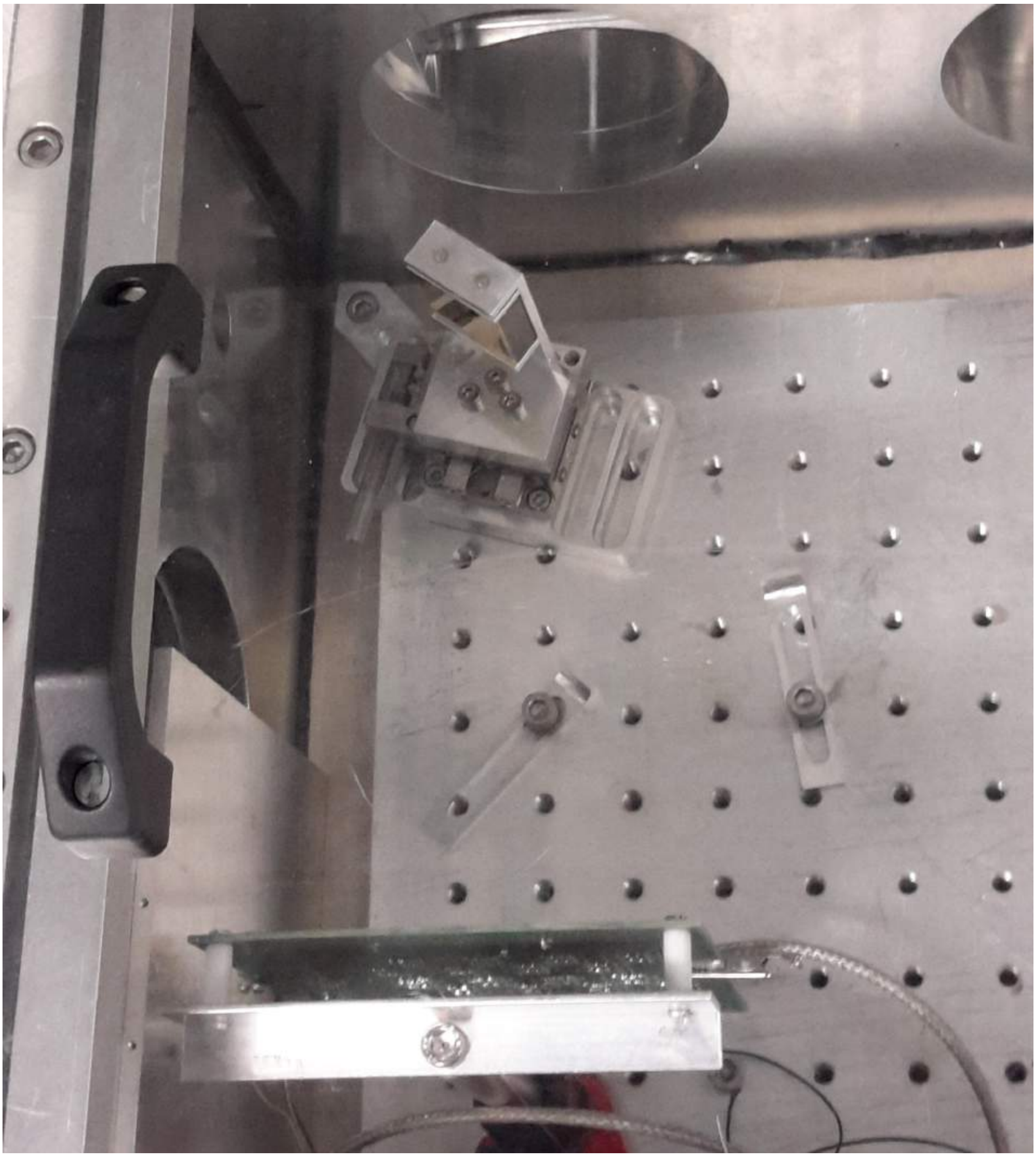

Figure 17: Profile measurement setup

The signal observed by the detector was changing with the power of the 4th harmonic which could be adjusted by varying pumping current of the laser. The signal pattern as a function of power is shown on Fig. 18. The most right distribution corresponds to the 0th order of the diffraction grating. The middle part corresponds to the 1st order of 85nm wavelength. The most left part is a 2d order of the 85nm wavelength.

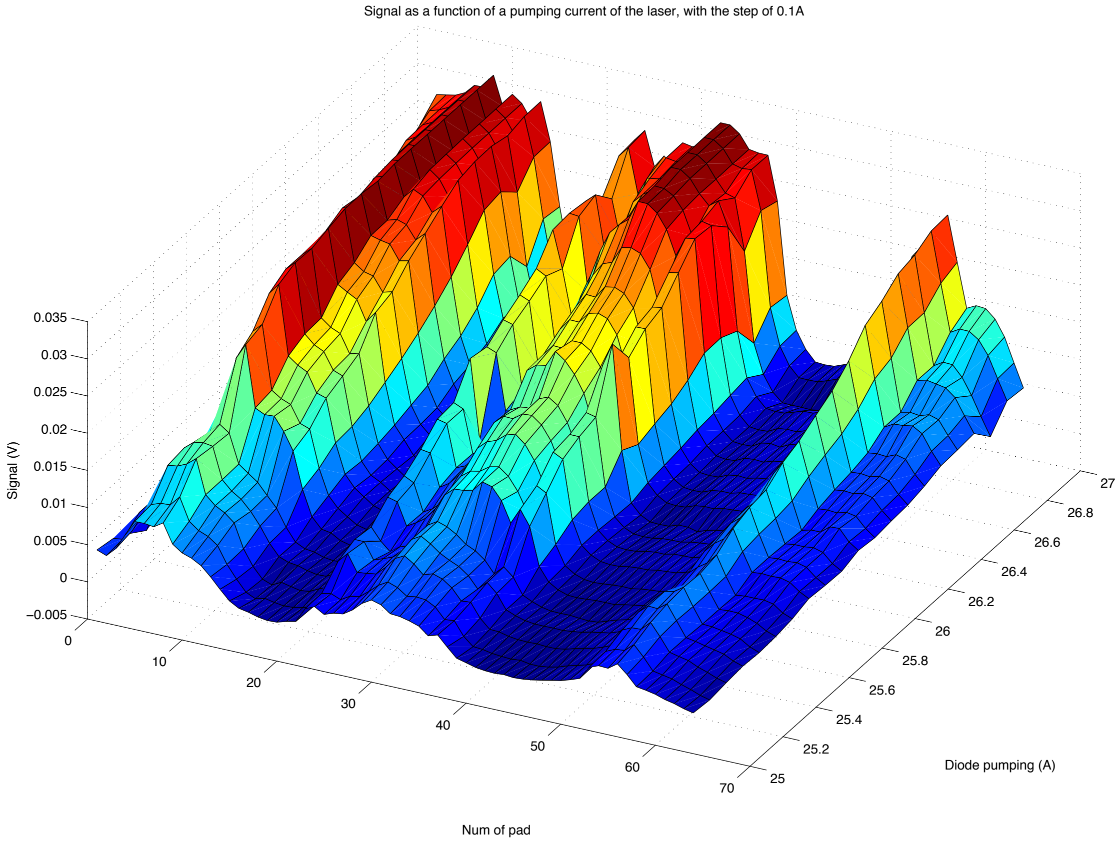

Figure 18: Signal as a function of power and number of the pad of the detector

At a low incident power (Fig. 19) one observes almost Gaussian distribution of peaks with a small wings visible by the side. However at a higher laser pumping of 26A one observes 3 peaks (Fig. 20). At a further pumping current of 27A saturation start to appear which eliminates 3 peak formation (Fig. 21).

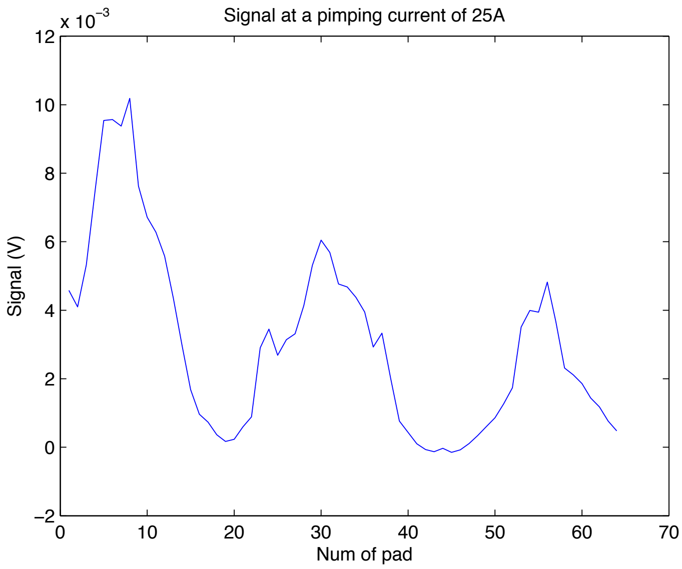

Figure 19: Signal as a function of the pad number of the detector

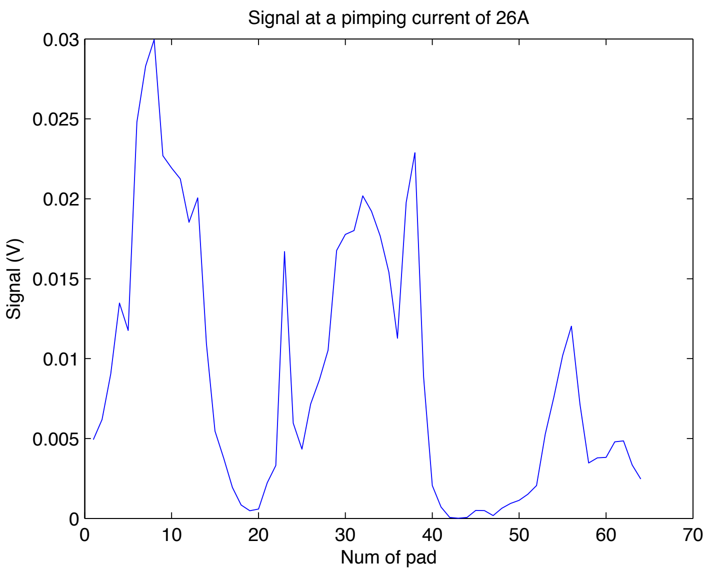

Figure 20: Signal as a function of the pad number of the detector

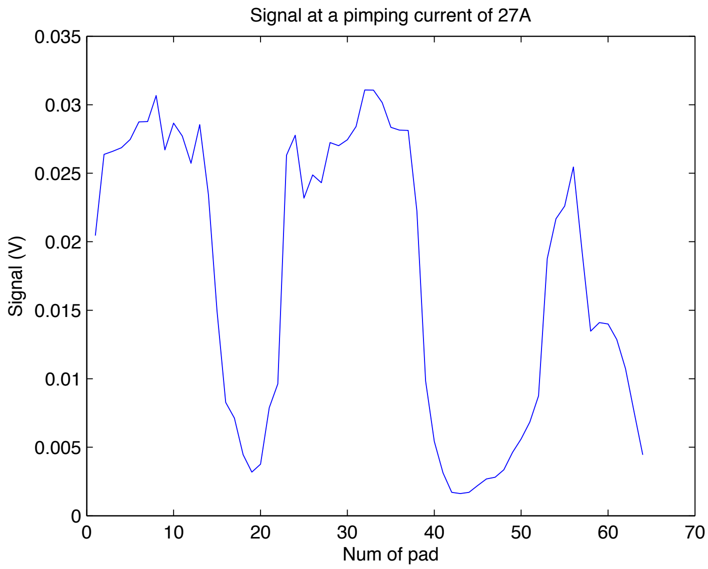

Figure 21: Signal as a function of the pad number of the detector

3.4 Profile measurement with the moving mirror

One more experiment of profile measurement was performed using the moving mirror. Experimental setup is shown on Fig. 22.

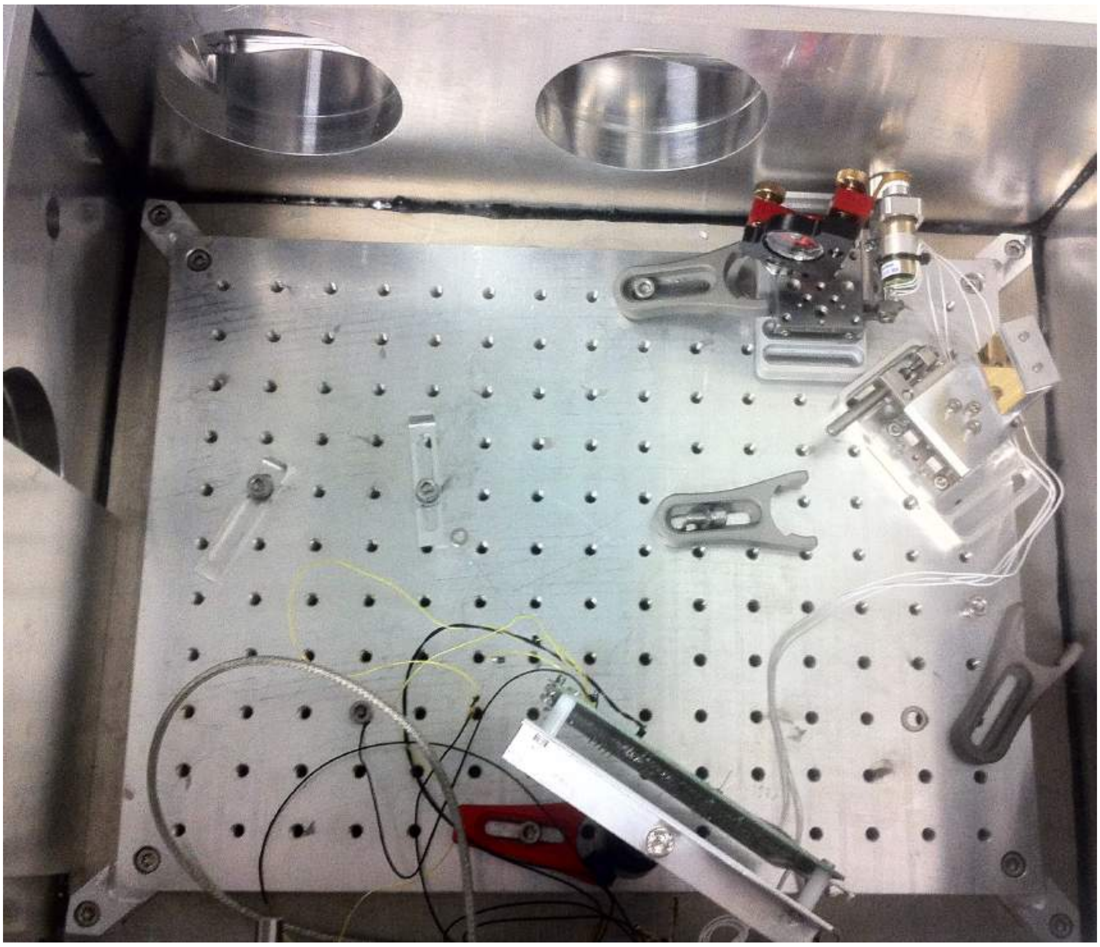

Figure 22: Experimental setup with moving mirror

It was found that the signal on oscilloscope depends on the position of the mirror. Which implies that beam diameter of the 85nm harmonic was greater than the surface area used for reflectance from the lens, hence the formation of the signal on oscilloscope depends on which part of the beam is reflected on the grating (Fig. 23, 24, 25).

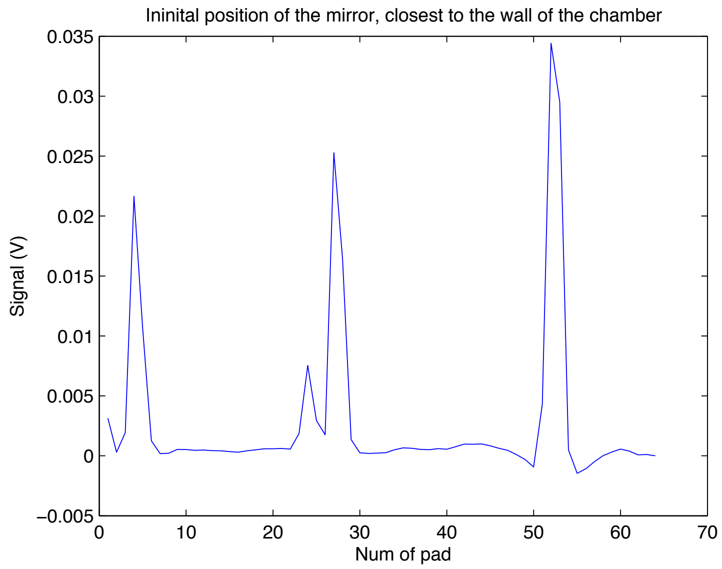

Figure 23: Signal as a function of the pad number of the detector

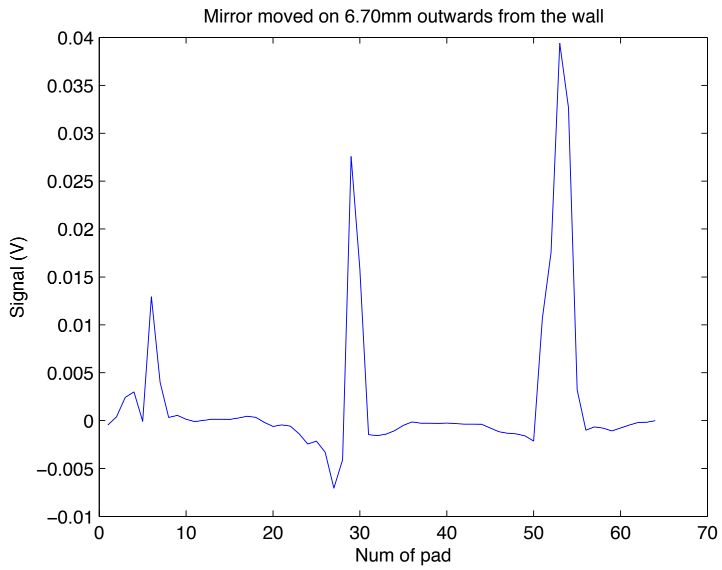

Figure 24: Signal as a function of the pad number of the detector

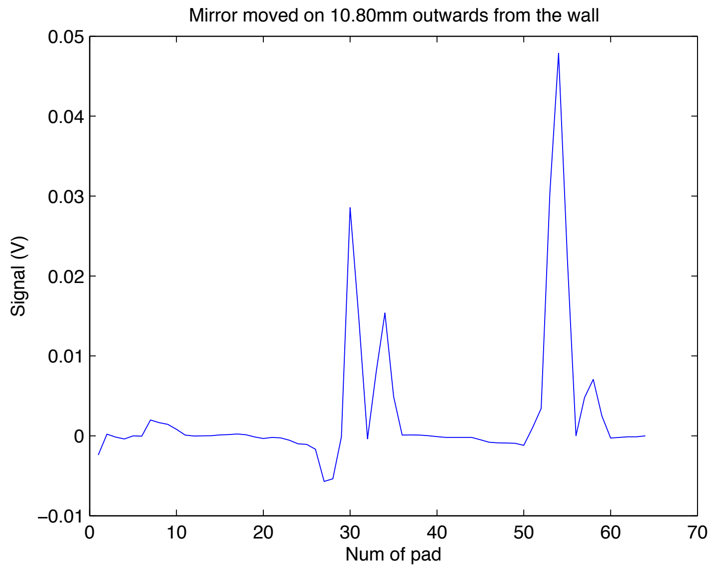

Figure 25: Signal as a function of the pad number of the detector

In fact, this experiment was done multiple times and 3 peaks were always observed. Depending on on the tilting angle of the lens and its position, different amount of beam profile is reflected into the grating. 3 peaks were also observed simultaneously.

3.5 Aluminum filter transmittance test

During the project aluminum film filters have been made in order make use of transmittance properties of the aluminum thin film. The thickness of the made filters was about 300nm. Experiments have been performed with this filter, however no light, neither for 85nm nor for 256nm was transmitted. Probably the filter was too thick.

3.6 Oscilloscope calibration

Oscilloscope is supposed to measure 64ms range which corresponds to 64 pads on the detector. However, the settings of oscilloscope have been done such that it measures the time period of 65ms, therefore the data which was acquired from the oscilloscope and processed later on assumed that there were 65 pads instead of 64. Hence, in fact, all previous measurements with the data from the oscilloscope have a small error, because oscilloscope measured 65ms instead of 64ms.

The settings of the oscilloscope were corrected, such that saved data provides measured data within 64ms period. Hence each 1ms corresponds to 1 pad.

3.7 Steady state condition

All experiments were performed at a steady state, meaning when the pressure inside the gas chamber and pressure inside the vacuum chamber stop to change.
Experiments at a non-steady state were also performed, however results are not included in the report, as change of signal was too fast to measure the dynamics precisely.
The typical indicated operational steady state pressure in the gas chamber for Argon was 750mbar (23mbar indicated on the detector). Typical steady state pressure of the vacuum chamber was $2 * 10^{-3}$mbar.
Before every experiment components were aligned such that at a pumping current of 35A the generated average power of the 4th harmonic (256nm) was not smaller than 230mW (typically 231mW).

3.8 Influence of differential pumping

From the beginning of the project differential pumping box was used, but later on removed. No difference in operation or signal detection was observed.

3.9 Beam alignment in the vacuum chamber

Intensity of the 85nm harmonic and profile strongly depends on the alignment of components. The proper alignment require to remove the gas chamber and the focusing lens before the gas chamber such that the 4th harmonic is entering the gas chamber without any obstacles. Make sure that the middle part of the beam profile is seen inside the vacuum chamber, and beam direction is straight and not deflected. Place a focusing lens back, make sure that the pattern in the vacuum chamber corresponds to the middle part of the beam.

3.10 Influence of thicker foil (20um)

Thicker foil of 20um was tested. The hole is burned at quite the same amount of pumping current as for the regular thin foil. Since the spatial jitter of the laser causes the expansion of the hole, it seems to be better to use the thicker film, as it will be less affected by the laser intensity. Probably it would be useful to test thicker films.
No significant changes in a detected signal was noticed while using thicker film.

3.11 Experiments with different gases

Influence of different gas media on double peak formation was performed. No changes have been done to the setup while measuring influence of different gases, except of a change of the gas medium.
Double peak formation occurs for all gases (Fig. 26, 27, 28), however with different efficiency due to the spectral properties of the used gases which affect efficiency of multiphoton absorption.

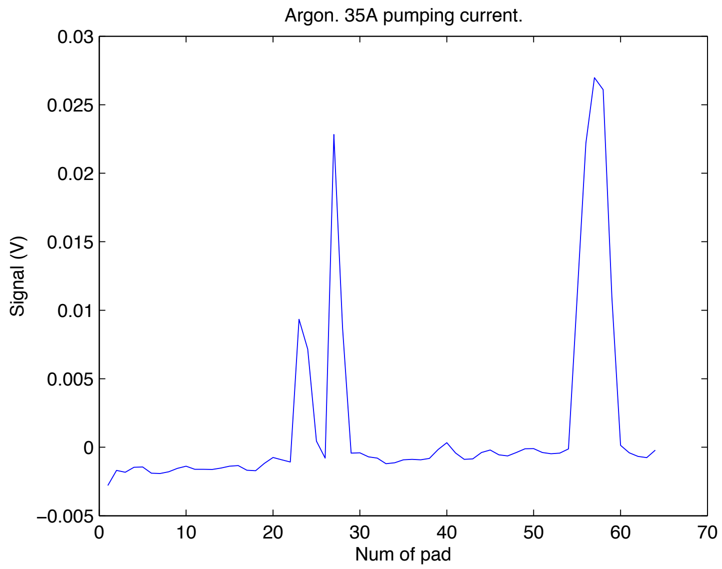

Figure 26: Signal as a function of the pad number

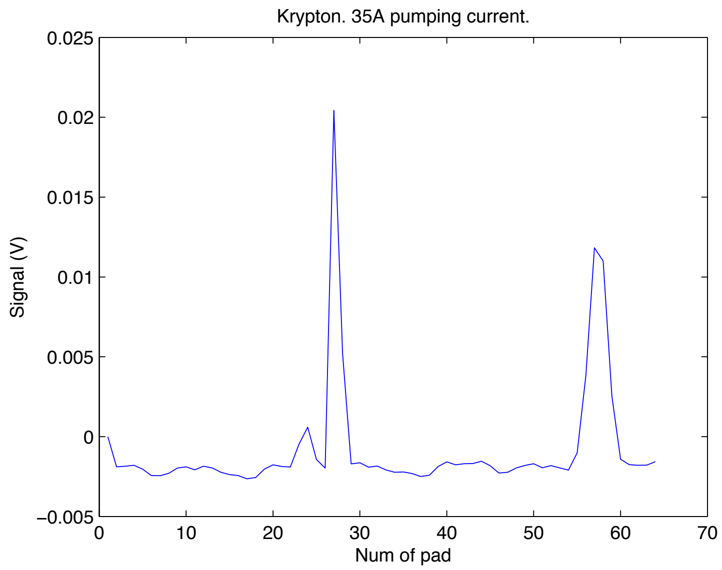

Figure 27: Signal as a function of the pad number

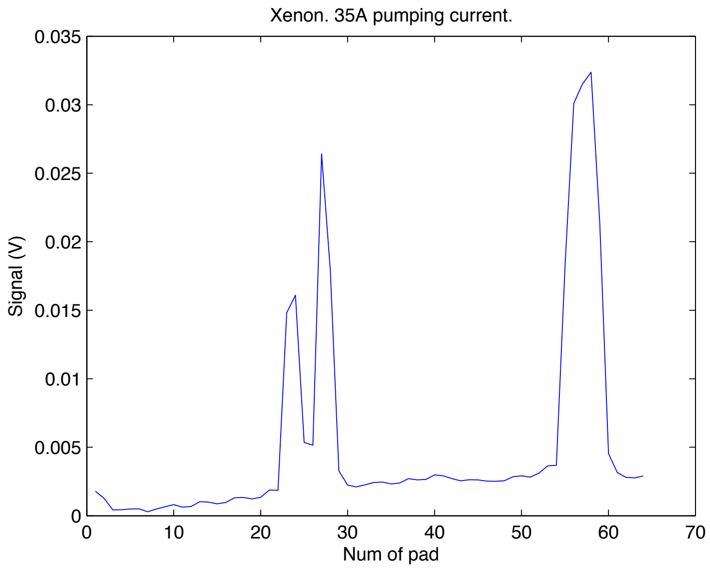

Figure 28: Signal as a function of the pad number

3.12 Diffraction pattern formation and stress

It was found that the diffraction fringes are formed for 4th harmonic which is used as a fundamental for generation of 85nm after it passes the hole in a foil (Fig. 29). Although the diameter of the 85nm harmonic and divergence of it should be smaller and hence the scale of the hole with respect to the 85nm harmonic is larger, nevertheless it is probable that the beam profile for 85nm has a similar diffraction pattern. This would explain formation of 3 peaks on the detector.

Figure 29: Fluorescence of 256nm harmonic from the white paper. The shot of the part of the beam is taken by external camera at some angle

In addition it was found that the diffraction pattern of 256nm wavelength is very sensitive to external vibrations and stress. In particular, pushing the vacuum chamber causes permanent change is the diffraction pattern ((Fig. 30)), due to the shift of the hole with respect to the laser beam and thus increase of the hole diameter.

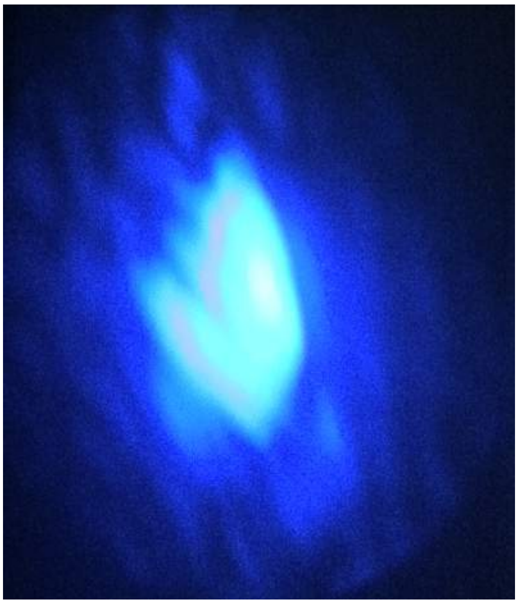

Figure 30: Fluorescence of 256nm harmonic from the white paper. The shot of the part of the beam is taken by external camera at some angle

Probably the same tendency applies to the 85nm harmonic. This would explain the disappearance of 3 peak formation after long time operation of the foil.

3.13 Saturation of the detector and retardation voltage

It was found that the saturation of the pad detector occurs, which restricts to measure signal at a high intensity, as the detector get saturated. Therefore not saturated signal was usually observed at a pumping current not higher than 25A.
The experiments with retardation voltage on the detector were performed. Signal indeed can be influenced by the retardation voltage, however this influence is insignificant, and probably gives a possibility to increase the pumping current of the laser up to 26A, but not higher, as saturation will occur again ((Fig. 31, 32, 33)). But it should be mentioned that the application of retardation voltage lowers the level of noise, and the signal becomes less distorted by noise (Fig. 33).

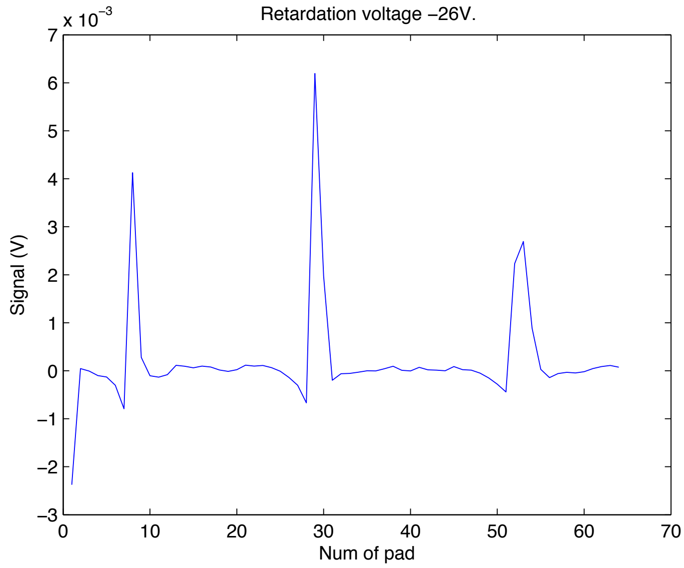

Figure 31: Signal as a function of the pad number

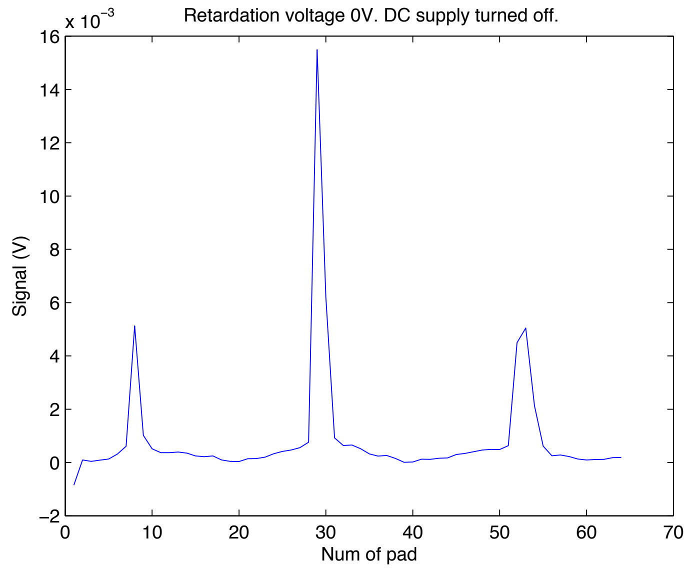

Figure 32: Signal as a function of the pad number

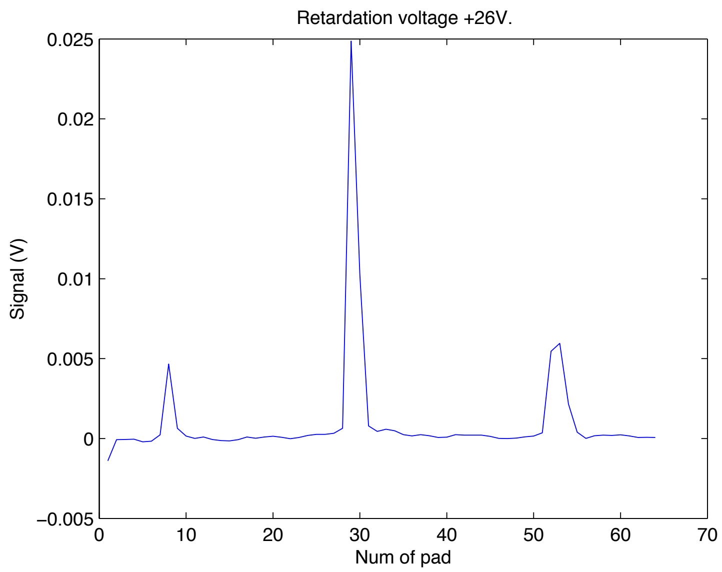

Figure 33: Signal as a function of the pad number

At the end of the project the problem of saturation was solved by covering the major part of the pads of the detector by the paper stripe (Fig. 34), leaving about 5 percents of the surface of each pad. In this case measurements without saturation can be performed for the whole range of pumping currents.

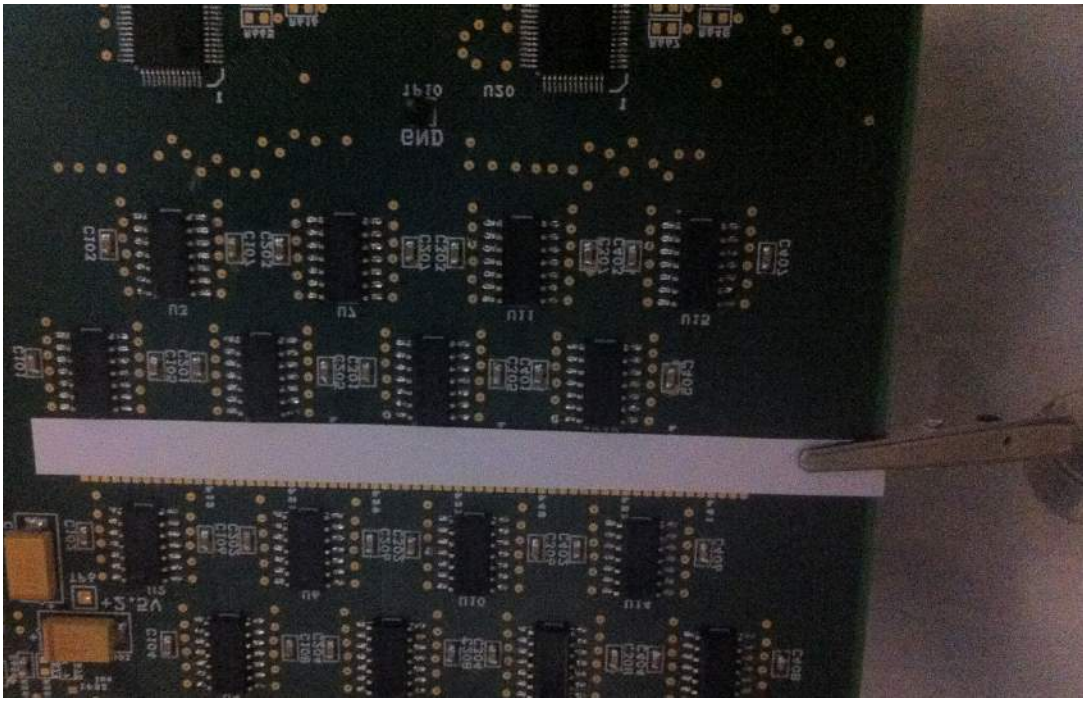

Figure 34: Paper stripe covering the surface of the detector pads

In addition, usage of the paper stripe which leaves only the small surface of each pad increased the resolution as the signal peaks become less smeared.
Influence of the 256nm harmonic on the golden pads was tested as well (Fig. 35).

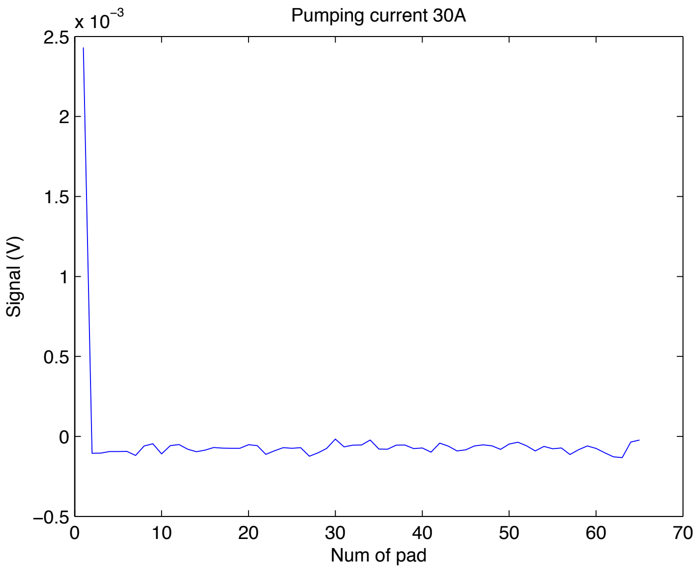

Figure 35: Peak corresponds to the 0th order of the grating

3.14 Experiment with the movement of vertically aligned pad detector

Experiments with the movement of vertically aligned pad detector were also performed. The observed pattern confirms the 3 peak formation.
However due to dimensions of the vacuum chamber and the detector, it was not possible to move the detector across the beam profile without tilting the detector. Hence due to geometrical issues it was not convenient to perform such experiments.

3.15 Positioning of the pad detector with respect to 1st mode

Initially positioning of the golden pad detector was such that the most right pad was at the position were the focusing of the 0th mode of the grating occurs [2].
However it has been noticed that the focal length for different modes is not the same. In particular the focal length for the 1st mode of 256nm harmonic is about twice larger than the focal length for the 0th mode.
Hence the new positioning of the detector was used, with respect to the 1st mode of 256nm harmonic. The detector was placed such that the most left pad of the detector was at the position where the focusing of the 1st mode of 256nm harmonic occurs. Hence the rest of the detector is exposed to the 1st and 2d modes of 85nm wavelength. However due to the smaller deviation angle and smaller divergence for the 85nm harmonic, focusing length for 85nm wavelength is shorter than for 256nm. This explains why signal of 85nm harmonic still occupies a couple of pads. Such a new positioning helped to increase the resolution and sharpness of detected peaks.

3.16 Power measurements.

Measurements of the amplitude of a signal as a function of power has been performed for 2 experimental setups. The results for the setup without mirror show how the signal changes with power, from only middle peak being detected up to the saturation (Fig. 18).
Measurements with better precision (Fig. 36) for the pumping power interval which does not cause saturation was performed for the experiment with the moving mirror in order to find the slope of how signal changes with incident on a gas intensity of 256nm harmonic. For the 3d harmonic generation, the slope should be approximately equal to 3 [2]. Mirror was positioned such that two peaks are clearly visible.

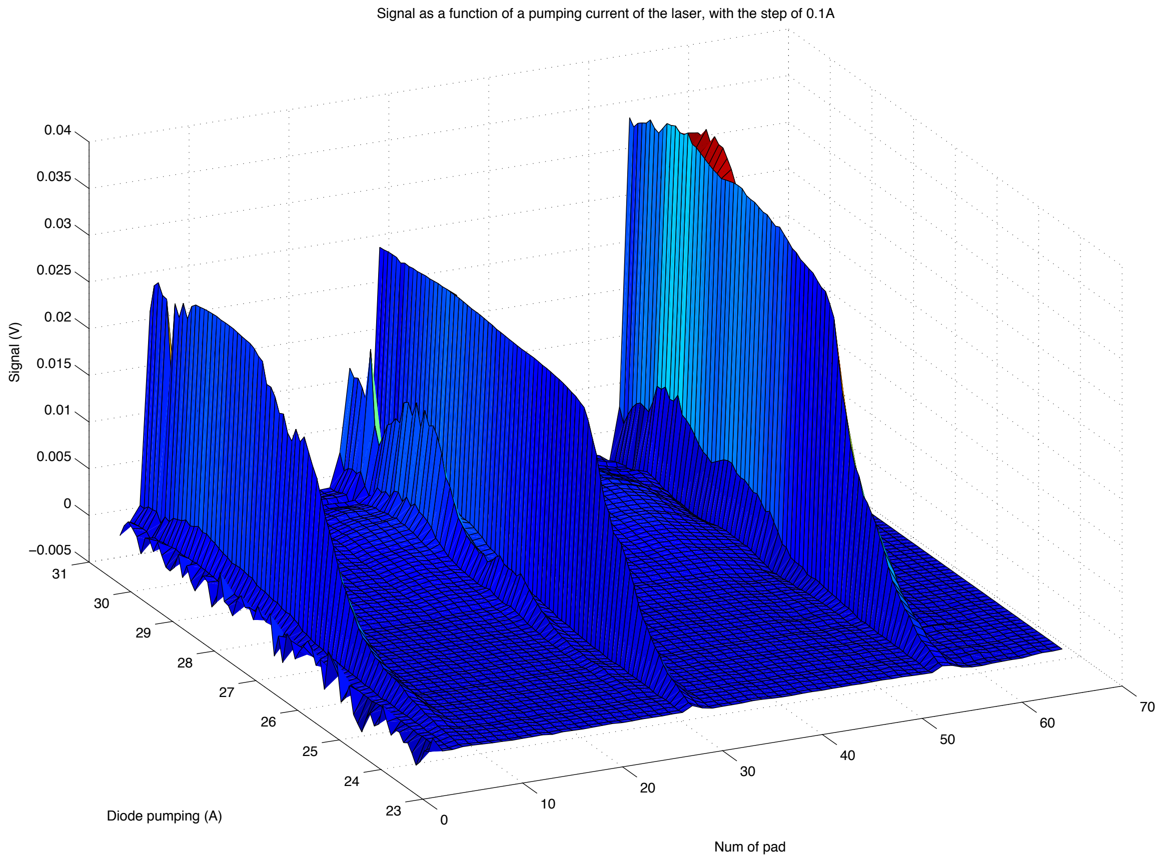

Figure 36: Signal as a function of the pad number of the detector and pumping of the laser

For the slope determination the average power of the 4th harmonic was measured (Fig. 37) as a function of laser pumping current with the detailed data at the end of this report.

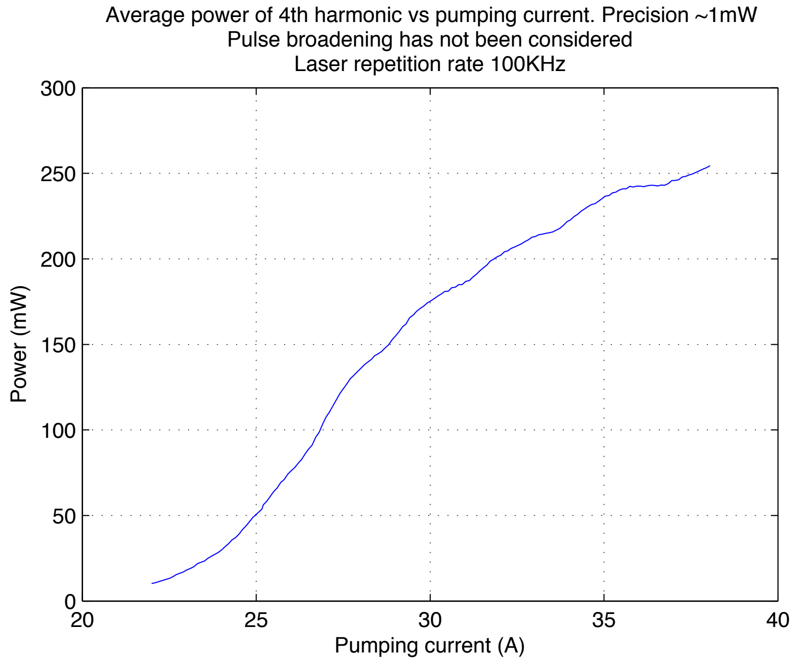

Figure 37: Average power as a function pumping current

The amplitude of the signal of the right peak as a function of a pumping current is shown on Fig. 38. The amplitude of the signal of the left peak as a function of a pumping current is shown on Fig. 39.

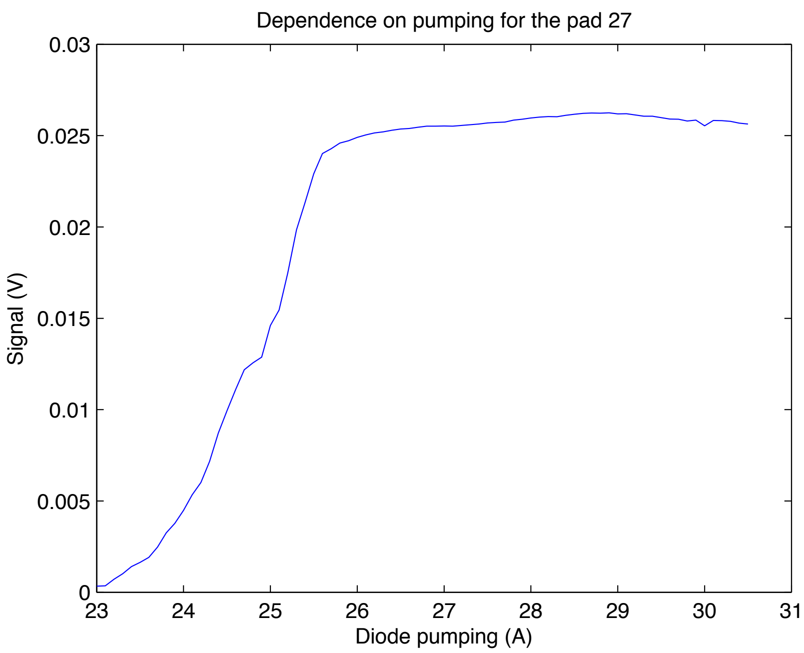

Figure 38: Amplitude of the signal as a function of pumping current for the right peak

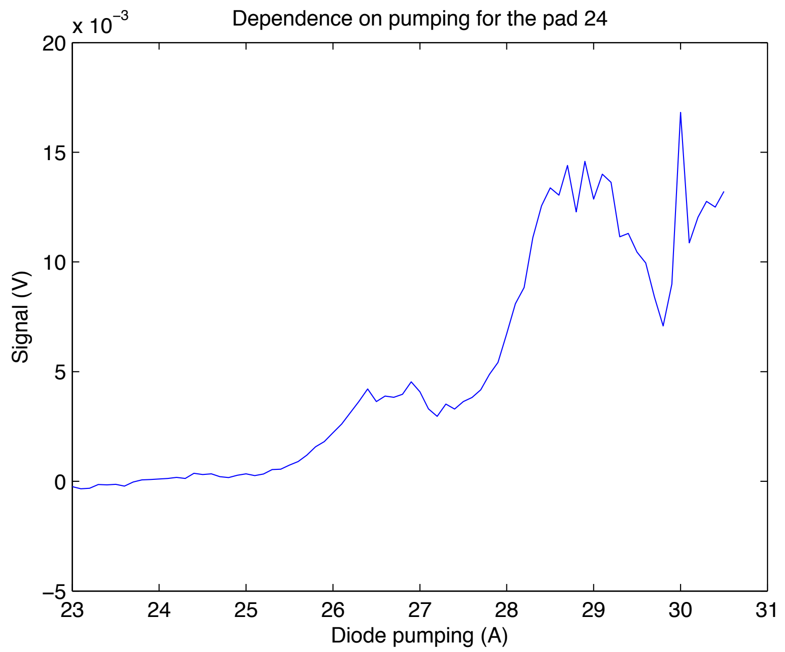

Figure 39: Amplitude of the signal as a function of pumping current for the left peak

The intermediate regions from both plots were taken for slope comparison. From the plot corresponding to the left peak the pumping current region [24.2;24.7] was taken while for the right peak the region of [28.0;28.5] was taken (Fig. 40, Fig. 41).

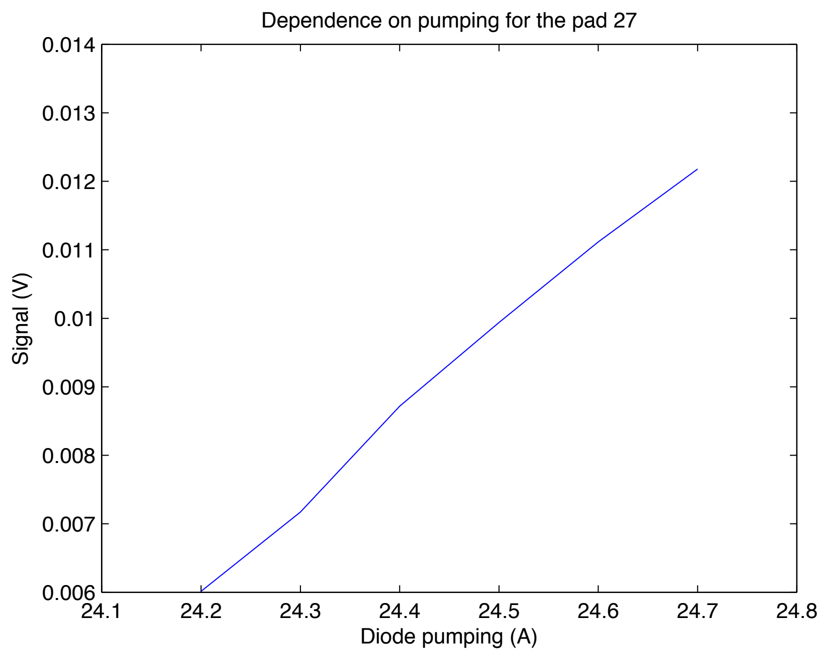

Figure 40: Interval from the plot of of the right peak

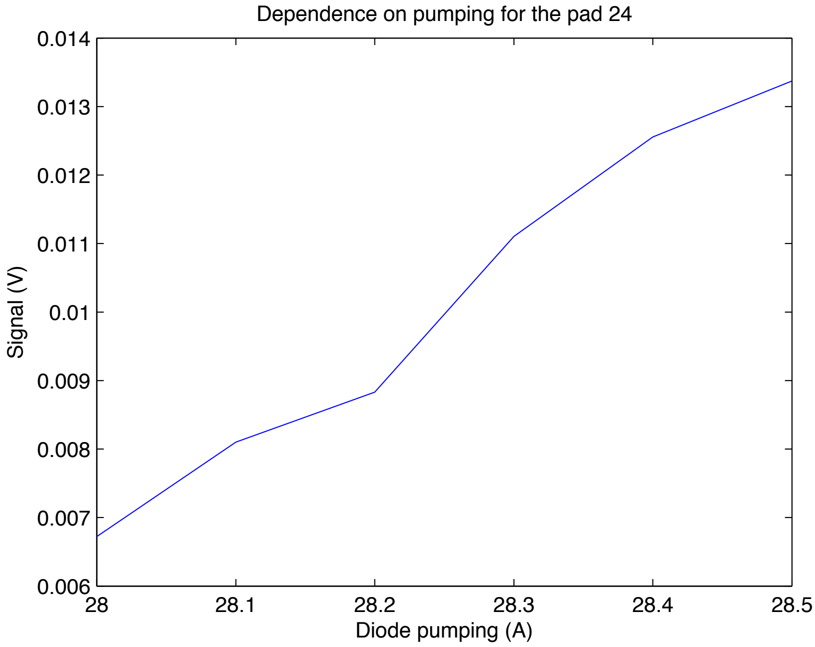

Figure 41: Interval from the plot of of the left peak

It was observed (Fig. 42, Fig. 43) that the slopes for to peaks are almost equal. This implies that two peaks should correspond to the same nonlinear order, hence both peaks must belong to the same harmonic.

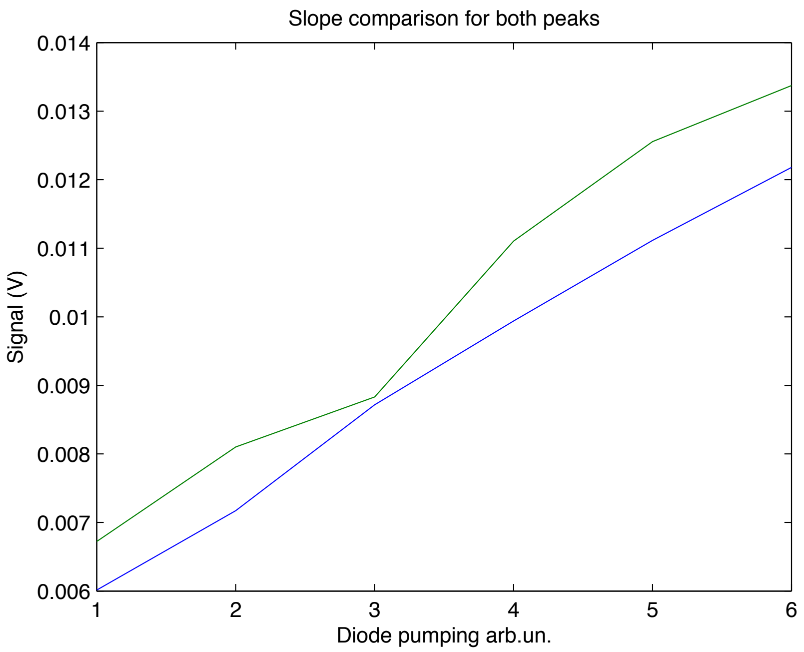

Figure 42: Slopes of functions for two peaks. Green curve corresponds to the left peak, blue curve corresponds to the right peak

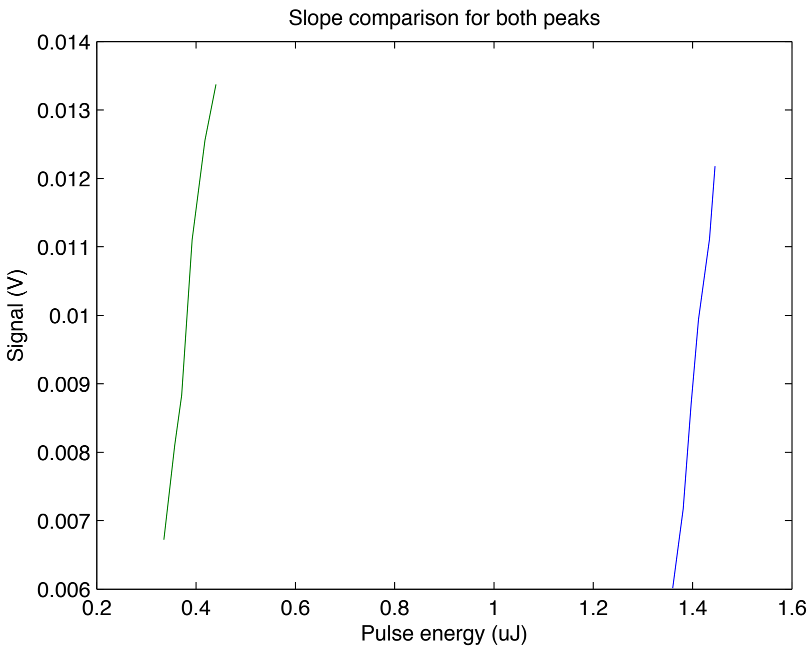

Figure 43: Slopes of functions for two peaks. Green curve corresponds to the left peak, blue curve corresponds to the right peak

3.17 Experiments with ring detector

Experiments with the round detector consisting of one pad covered by the gold foil were also performed. It was noticed that saturation also happens for this detector. However it is possible to move the grid further away from the golden foil, which, with the usage of the retardation voltage should reduce the amount of electrons which hit the grid. However this adjustment has not been done.
There were also experiments with the retardation voltage, however the presence of the retardation voltage of 26V (maximum voltage of DC supply) did not have a significant influence. Probably the grid must have been moved further.
Also signal on the ring detector experience high timing jitter with the amplitude of about 30 percents of the signal, which does not allow to perform precise measurements.

4 Conclusion and Proposals

The multiple peak formation occurs for all gases, this contradicts arguments for non-linear explanation of multiphoton absorption of photons of 4th harmonic and 2d harmonic. In addition, change of the signal depending on the position of the mirror placed before the grating implies that the formation of peaks is not a spectral effect, but rather effect of the profile. The presence of the same slope of change of a signal as a function of pulse energy for 2 peaks also confirm that 2 peaks should be of one wavelength.
Hence it is quite unlikely that multiple peak formation is a spectral effect.

Beam profile of the 4th harmonic was measured [2] and found to be Gaussian, hence formation of multiple peaks is not due to the multiple mode profile of 4th harmonic.
Thus, three multiple peak formation is either due to the ring profile formation of 85nm due to phase matching during the generation of 12 harmonic or effect of the diffraction of the hole. Since the diffraction fringes for 256nm were observed it is probable that there will be also diffraction fringes formation for 85nm harmonic. It was also observed that the multiple peak formation eliminates with expansion or deformation of the hole, while ring profile formation due to phase matching should not be affected by the hole distortion. Hence I conclude that most probable occurrence of multiple peak formation is an effect of diffraction from the hole in a foil.
However more than 3 peaks were never observed. In case of the diffraction pattern, there must be multiple peaks. But the absence of more than 3 peaks is probably due to the low intensity of higher order peaks.

- Fluorescence properties of C_2H_2 in a range of 50-106nm have been reported [5]. In this case, it would be possible to convert XUV wavelength ranges into visible range for further detection. However in order to use C_2H_2 as a detector one has to store it in a liquid or solid form, which seems to be not possible in a vacuum environment.

- The problem of saturation of the detector have to be resolved, otherwise it limits the ability of measurements. Application of retardation voltage although has an effect, but not significant

- The polarization of the 4th harmonic of 256nm has to be checked. As indicated on Fig. 4 the reflectance from the quartz lens used as a mirror strongly depends on polarization of incident light.

- It is possible instead of quartz lens which acts as a mirror to use a lens of another material placed at a Brewster angle. The property of material have to be such that for Brewster angle for 256nm this material has relatively high reflectivity for 85nm. In this case 85nm will be reflected, although 256 will be transmitted. Therefore this lens will act as a filter for 85nm harmonic.

- It seems that the conversion of the intensity on the pad into electrical signal is not linear. It also seems that doubling the intensity does not double the signal. Therefore there is a need to calibrate the detector in order to get a calibrational curve to which further measurements can be referred. Otherwise any measurements can not be considered correct.

- During the measurements with the grating it has been noticed that the signal reflected from the mirror affects only about 20 percents of the surface of the grating. However the larger the affected area, the narrower are the diffraction peaks. Also, the incident on a grating beam is not collimated, which also causes the broadening of diffraction peaks. Therefore the intention should be to affect as larger area as possible with as collimated beam as possible. It is better to perform focusing of the diffracted beam from the grating, rather than before the grating.

References

[1] Datenblatt JenLas D2.fs, 2009. *JENOPTIK Laser, Optik, Systeme GmbH*

[2] Erzeugung Harmonischer niedriger Ordnung aus fs-UV-Laserpulsen. *Johanna Ratzek, Bachelor thesis, University of Hamburg, 2015*

[3] Aufbau einer hochrepetierenden XUV-Lichtquelle mittels Hohe-Harmonischen-Erzeugung. *Dominic Laumer, Bachelor thesis, University of Hamburg, 2015*

[4] IMD database. *David Windt*

[5] Fluorescence from photoexcitation of C2H2 at 50-106nm. *J.C.Han, Chao Ye. The Journal of Chemical Physics. 1989. doi: 10.1063/1.455810*

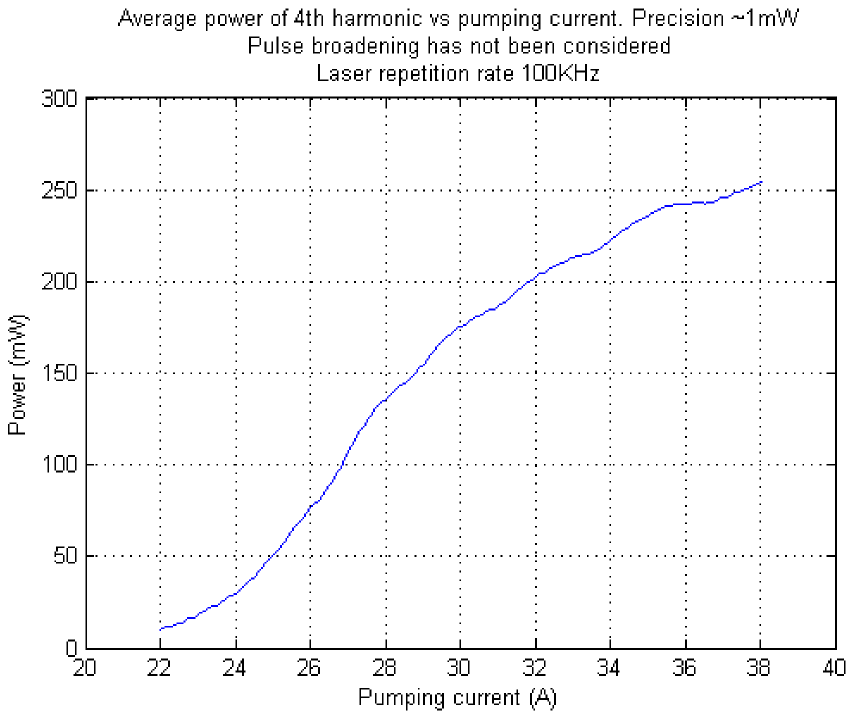

Pumping current (A)	Average power (mW)	Pulse Power (GW)	Pulse Energy (uJ)
21,991	10,200	0,255	0,102
22,094	10,700	0,268	0,107
22,194	11,300	0,283	0,113
22,292	11,900	0,298	0,119
22,392	12,500	0,313	0,125
22,496	13,200	0,330	0,132
22,595	14,100	0,353	0,141
22,693	15,300	0,383	0,153
22,797	16,200	0,405	0,162
22,898	16,900	0,423	0,169
22,999	18,100	0,453	0,181
23,102	19,000	0,475	0,190
23,204	20,000	0,500	0,200
23,307	21,800	0,545	0,218
23,409	22,600	0,565	0,226
23,511	23,400	0,585	0,234
23,612	25,000	0,625	0,250
23,712	26,200	0,655	0,262
23,811	27,300	0,683	0,273
23,907	28,300	0,708	0,283
24,007	29,900	0,748	0,299
24,106	31,800	0,795	0,318
24,207	33,500	0,838	0,335
24,304	35,700	0,893	0,357
24,406	37,100	0,928	0,371

24,508	39,200	0,980	0,392
24,606	41,800	1,045	0,418
24,706	44,000	1,100	0,440
24,804	46,300	1,158	0,463
24,902	48,800	1,220	0,488
25,002	50,600	1,265	0,506
25,163	53,700	1,343	0,537
25,203	56,200	1,405	0,562
25,301	58,300	1,458	0,583
25,400	61,000	1,525	0,610
25,502	63,900	1,598	0,639
25,602	66,100	1,653	0,661
25,705	69,300	1,733	0,693
25,805	71,000	1,775	0,710
25,908	74,200	1,855	0,742
26,010	76,200	1,905	0,762
26,112	78,100	1,953	0,781
26,210	80,700	2,018	0,807
26,311	82,900	2,073	0,829
26,411	86,200	2,155	0,862
26,510	88,900	2,223	0,889
26,607	91,100	2,278	0,911
26,711	95,900	2,398	0,959
26,810	98,700	2,468	0,987
26,911	103,600	2,590	1,036
27,009	107,600	2,690	1,076
27,107	110,500	2,763	1,105
27,206	114,100	2,853	1,141
27,305	117,700	2,943	1,177
27,406	121,200	3,030	1,212
27,507	124,200	3,105	1,242
27,604	126,900	3,173	1,269
27,704	130,000	3,250	1,300
27,804	131,800	3,295	1,318
27,905	133,900	3,348	1,339
28,007	136,000	3,400	1,360
28,111	138,100	3,453	1,381
28,209	139,700	3,493	1,397
28,307	141,200	3,530	1,412
28,409	143,400	3,585	1,434
28,509	144,500	3,613	1,445
28,608	145,900	3,648	1,459
28,707	148,000	3,700	1,480
28,806	149,700	3,743	1,497
28,911	152,900	3,823	1,529
29,012	155,000	3,875	1,550

29,109	157,400	3,935	1,574
29,209	160,400	4,010	1,604
29,308	161,900	4,048	1,619
29,411	165,500	4,138	1,655
29,512	167,100	4,178	1,671
29,616	169,400	4,235	1,694
29,715	171,100	4,278	1,711
29,816	172,400	4,310	1,724
29,918	174,200	4,355	1,742
30,018	175,400	4,385	1,754
30,119	176,800	4,420	1,768
30,210	178,100	4,453	1,781
30,320	179,500	4,488	1,795
30,420	180,900	4,523	1,809
30,523	181,200	4,530	1,812
30,622	183,100	4,578	1,831
30,723	183,400	4,585	1,834
30,823	184,900	4,623	1,849
30,923	185,000	4,625	1,850
31,024	186,900	4,673	1,869
31,126	187,300	4,683	1,873
31,230	189,400	4,735	1,894
31,332	191,000	4,775	1,910
31,430	193,000	4,825	1,930
31,529	194,700	4,868	1,947
31,627	196,300	4,908	1,963
31,728	198,600	4,965	1,986
31,829	199,900	4,998	1,999
31,931	201,200	5,030	2,012
32,033	202,200	5,055	2,022
32,134	204,100	5,103	2,041
32,233	204,700	5,118	2,047
32,331	206,100	5,153	2,061
32,431	207,000	5,175	2,070
32,529	207,900	5,198	2,079
32,629	208,800	5,220	2,088
32,726	210,100	5,253	2,101
32,829	211,200	5,280	2,112
32,928	212,700	5,318	2,127
33,028	213,100	5,328	2,131
33,128	214,100	5,353	2,141
33,228	214,400	5,360	2,144
33,330	215,000	5,375	2,150
33,430	215,300	5,383	2,153
33,532	215,800	5,395	2,158
33,631	216,800	5,420	2,168

33,731	217,900	5,448	2,179
33,834	219,600	5,490	2,196
33,934	221,700	5,543	2,217
34,037	222,900	5,573	2,229
34,139	224,700	5,618	2,247
34,242	226,100	5,653	2,261
34,338	227,900	5,698	2,279
34,440	229,200	5,730	2,292
34,539	230,600	5,765	2,306
34,639	231,700	5,793	2,317
34,742	232,300	5,808	2,323
34,840	233,700	5,843	2,337
34,940	235,100	5,878	2,351
35,043	236,700	5,918	2,367
35,141	237,000	5,925	2,370
35,242	238,600	5,965	2,386
35,339	239,000	5,975	2,390
35,441	240,200	6,005	2,402
35,540	241,000	6,025	2,410
35,639	241,000	6,025	2,410
35,740	242,400	6,060	2,424
35,838	242,000	6,050	2,420
35,942	242,500	6,063	2,425
36,042	242,500	6,063	2,425
36,140	242,200	6,055	2,422
36,242	242,700	6,068	2,427
36,343	243,000	6,075	2,430
36,447	242,900	6,073	2,429
36,547	242,600	6,065	2,426
36,643	243,100	6,078	2,431
36,746	243,000	6,075	2,430
36,846	244,000	6,100	2,440
36,948	245,800	6,145	2,458
37,048	245,900	6,148	2,459
37,147	246,300	6,158	2,463
37,248	247,800	6,195	2,478
37,350	248,300	6,208	2,483
37,451	249,100	6,228	2,491
37,551	249,700	6,243	2,497
37,649	250,600	6,265	2,506
37,751	251,600	6,290	2,516
37,847	252,500	6,313	2,525
37,950	253,300	6,333	2,533
38,051	254,500	6,363	2,545